X-ray Observations of Cataclysmic Variables

Manabu ISHIDA
Tokyo Metropolitan University

Outline

- Introduction to X-ray Astronomy
  - ✓Instrumentation
- Plasmas treated in X-ray Astronomy
  - ✓Coronal approximation
- Cataclysmic Variables
  - ✓Dwarf Novae (non-magnetized)
  - ✓Polars and Intermediate Polars (magnetized)
- Future Japanese Mission

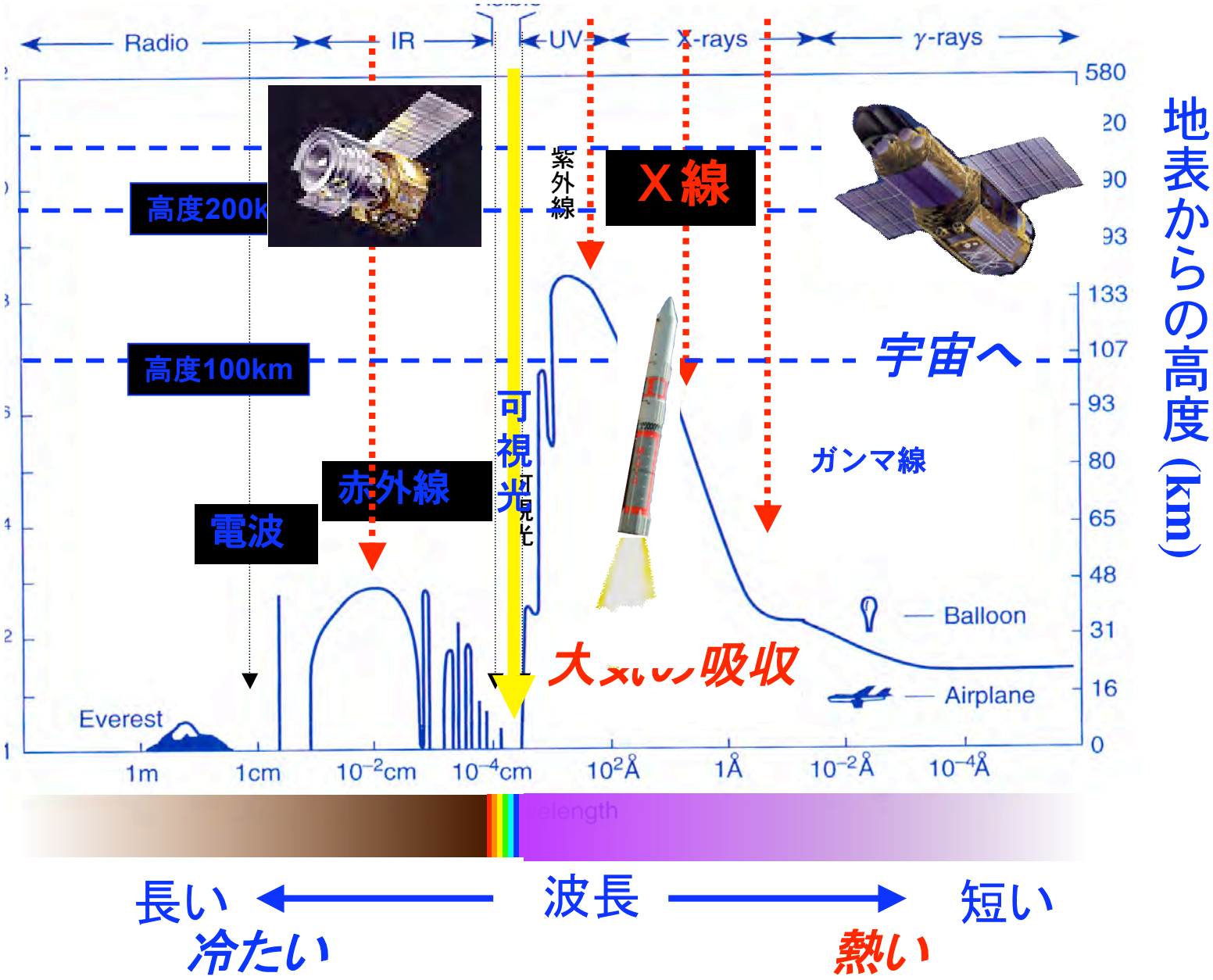
Radio
IR
UV
X-rays
γ-rays
580
20
90
93
133
107
93
80
65
48
31
16
0
高度200k
高度100km
紫外線
X線
宇宙へ
可視光
赤外線
電波
ガンマ線
Balloon
Airplane
Everest
大気の吸収
1m
1cm
10⁻²cm
10⁻⁴cm
10²Å
1Å
10⁻²Å
10⁻⁴Å
長い
波長
短い
冷たい
熱い
地表からの高度(km)

X-ray Missions in the 21st Century

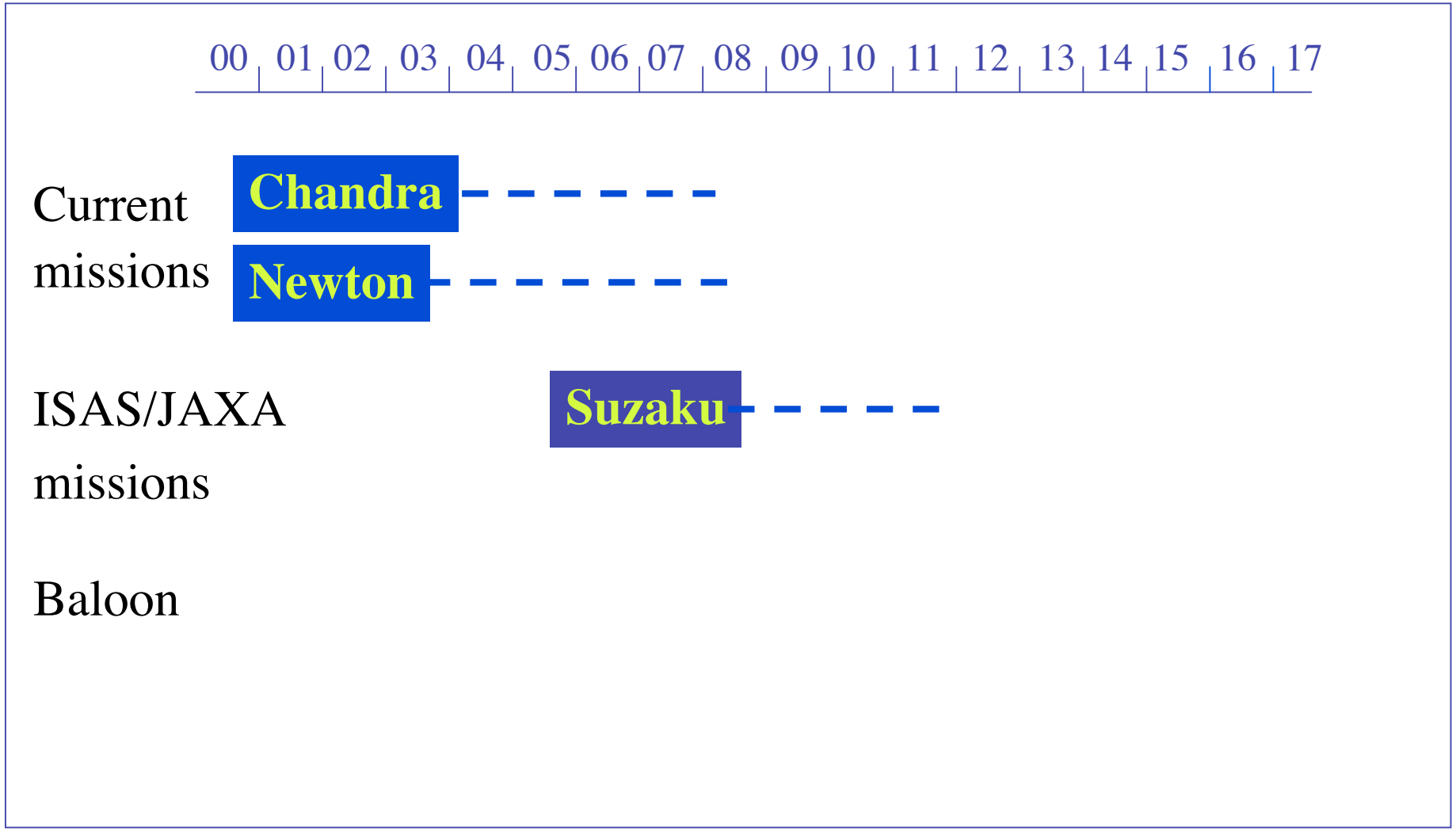

Instrument: X-Ray Telescope (XRT)

- Normal-incident optics does not work because of absorption.
- Refractive index of metal is slightly smaller than unity.
  - ⇨ Total reflection with a grazing angle of $\theta < 1°$.

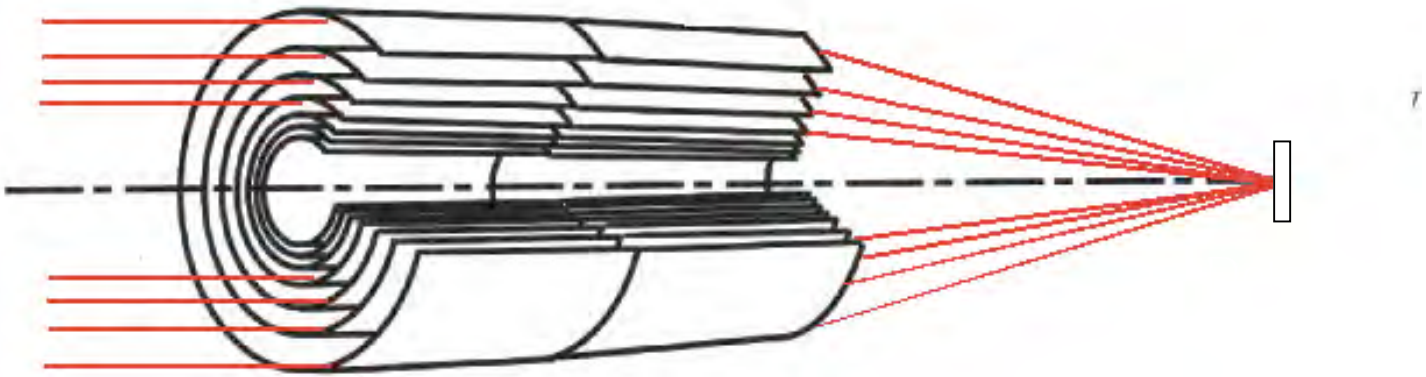

- Grazing-incidence optics is inefficient because $A_{eff} << A_{geo}$.
  - ⇨ Thin-foil-nested Optics
- Merits of adopting the telescope.
  - ✓ Imaging
  - ✓ Low-background → improvement of sensitivity.

Instrument: Charge-Coupled Device

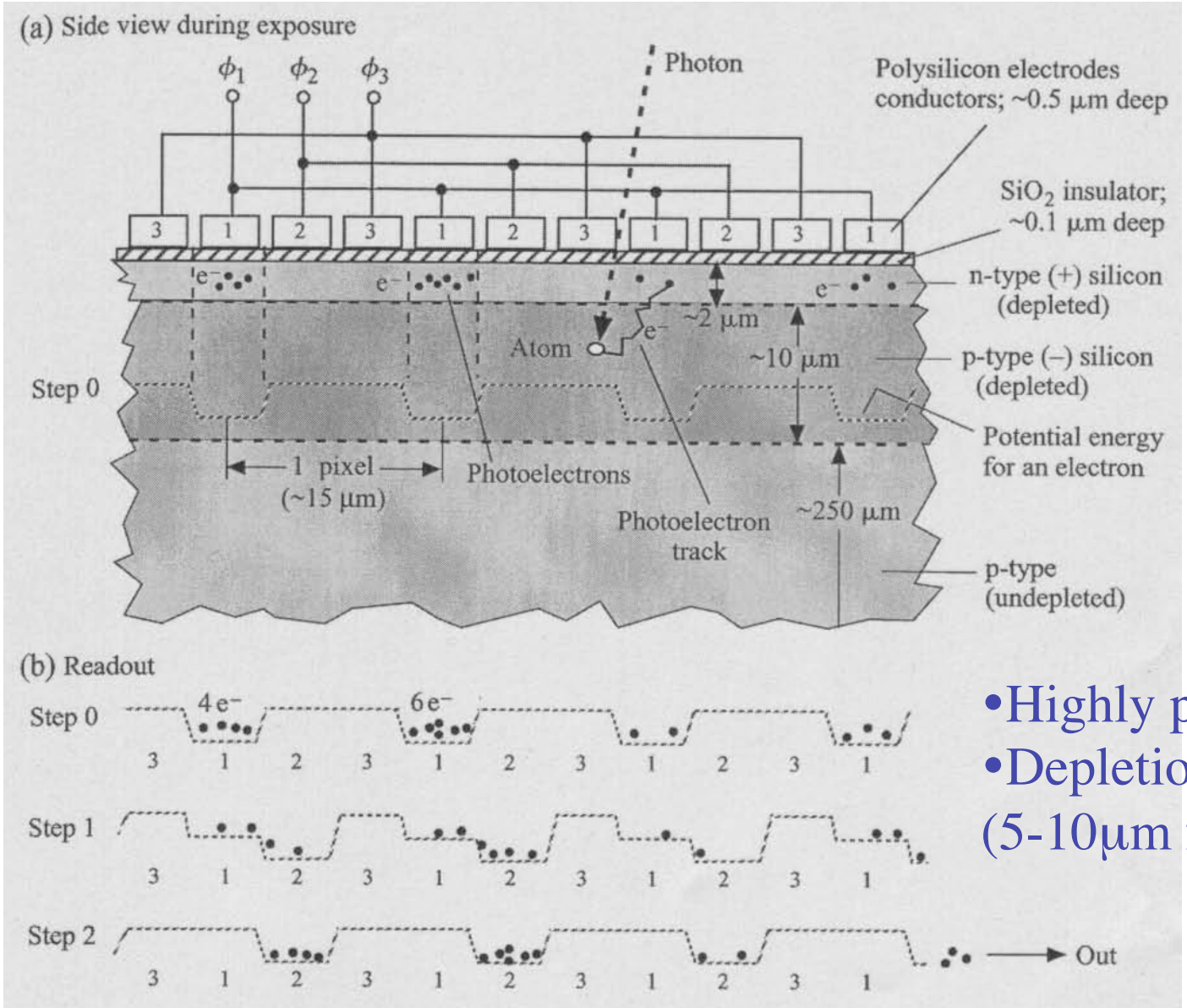

- Highly pure Si crystal
- Depletion layer ~ 70μm (5-10μm for Optical)

The Suzaku Observatory

- Launched into a nearly circular LEO orbit (inc.=31deg, alt.=570 km) with the M-V rocket (ISAS/JAXA)
- W = 1.7 tons
- Japan-US collaboration

X-ray Telescopes

XRT
NASA/GSFC-Nagoya-
ISAS/JAXA

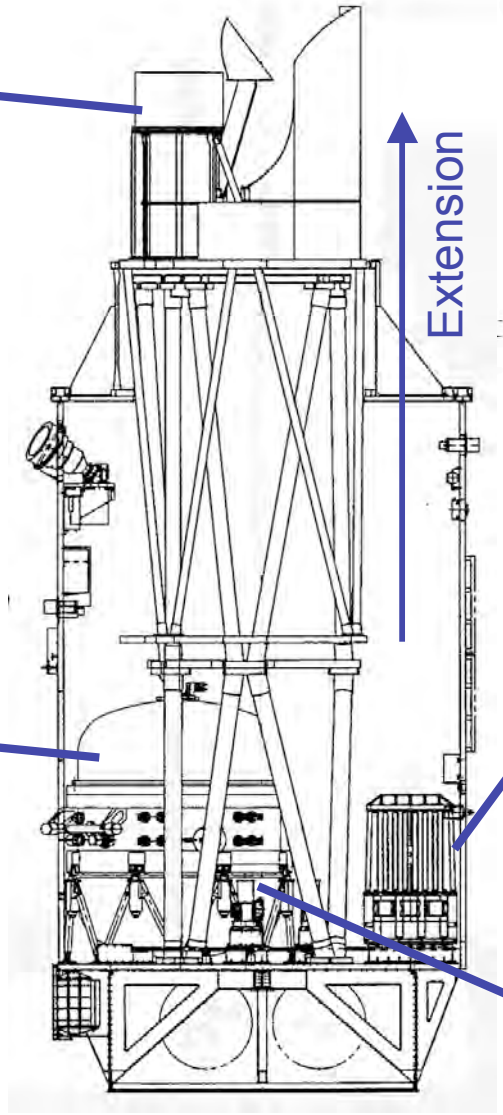

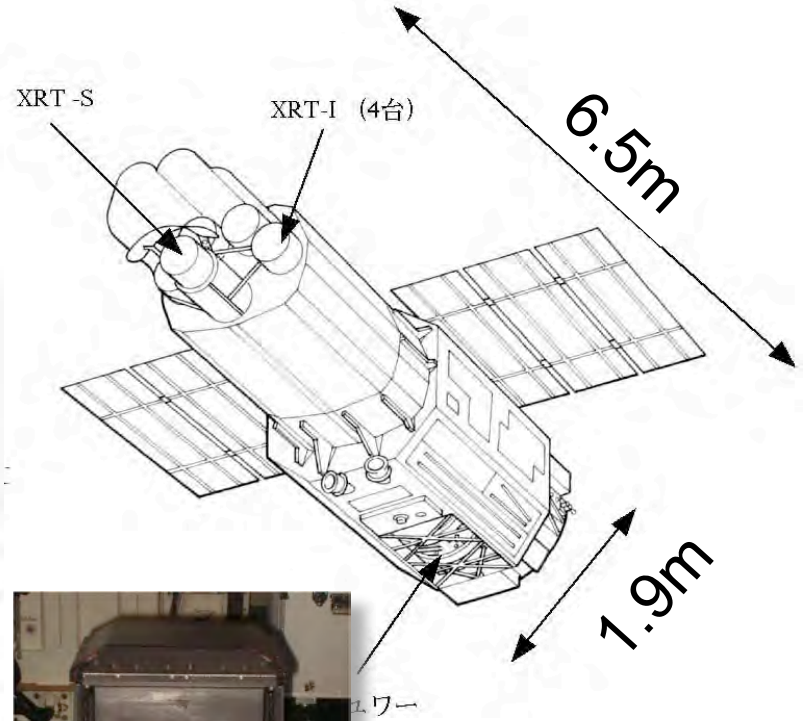

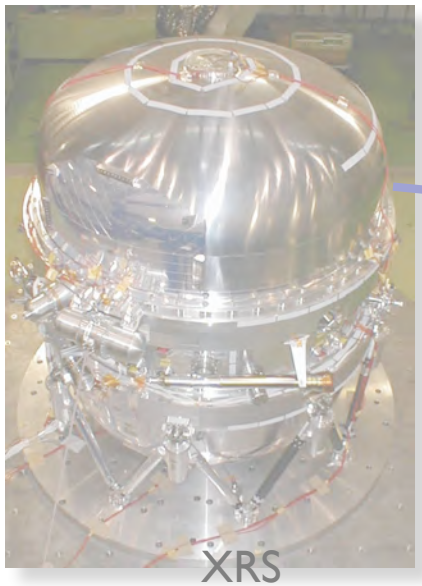

XRS
NASA/GSFC-Wisconsin
-ISAS/JAXA-TMU

X-ray micro calorimeter

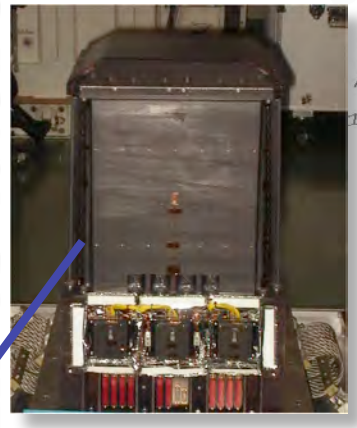

Hard X-ray detector
HXD
Tokyo-ISAS/JAXA-
Riken-Saitama-
HIroshima-Kanazawa-...

X-ray CCD camera
(4 modules)
XIS
MIT-Kyoto-Osaka -
ISAS/JAXA-.....

X-ray CCD camera (XIS)

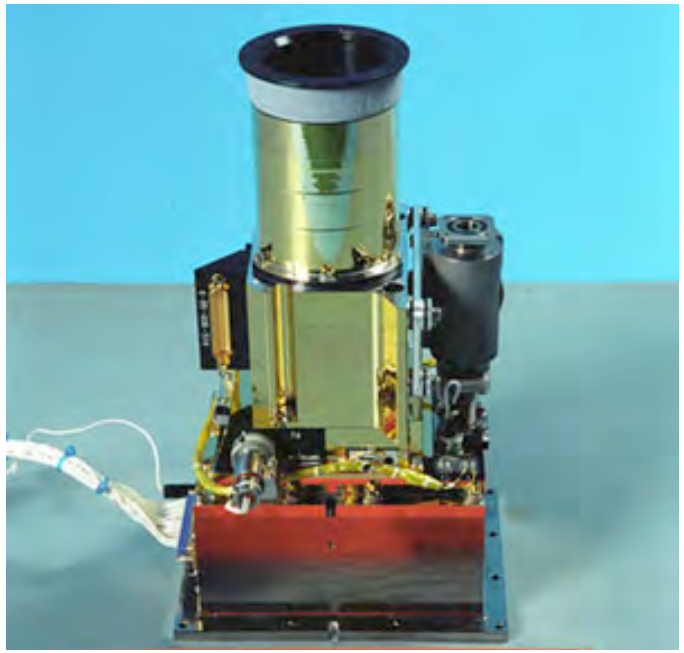

Focal plane assembly

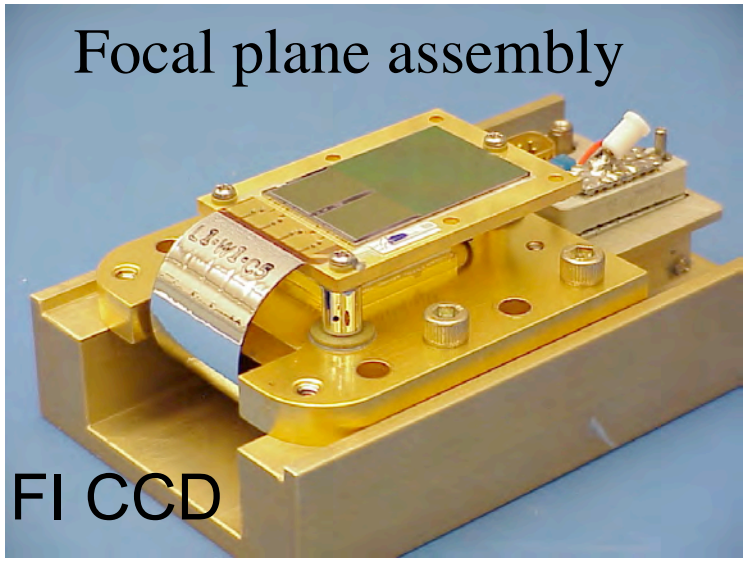

FI CCD

4 CCD cameras

- 3 sets of FI (front-side illuminated) CCD
- 1 set of BI (back-side illuminated) CCD

Manufacturer	MIT LL, CCID41
Architecture	3-phase, FT
Pixel size	24x24μm
Format	1024x1026 (imaging area)
FOV	18'x18'
Depletion layer	70μm (FI)
Readout time	8 sec (nominal)
Oper. Temp	−90°C
Energy range	0.2 - 12 keV
ΔE	~140eV(@6keV)

Developed by MIT, Kyoto Univ, Osaka Univ, ISAS/JAXA, etc.

The Hard X-ray Detector (HXD)

- collimated detector
- wide band-pass of 8-600keV by the combination of GSO and Si-PIN
- tight active shielding with well-type BGO

Energy range
2 mm^{t} Si-PIN : 8-60 keV
5 mm^{t} GSO(/BGO phoswitch)
40-600 keV

FOVs
<100 keV : 0.55^{o} (FWHM)
>100 keV : 4.5^{o} (FWHM)

Time resolution = 61 μs

Plasma Treated in X-ray Astronomy

- Non-thermal emission ($E > 10$keV):
  - ✓ Synchrotron Emission (B ~ μG)
  - ✓ Inverse Compton (CMB photons etc.)
  - ✓ Non-thermal bremsstrahlung (Collision of particle with molecular cloud)

    Pulsar, Active Galactic Nuclei.
  - ✓ Photoionized Nebula Emission ($E < 10$keV) : Cloud irradiated by an intense X-ray source (6.4keV Iron fluorescent K_α line).

    Star forming region, Accreting compact binaries.
- Thermal Emission ($E < 10$keV)
  - ✓ Blackbody radiation (optically thick): accretion disk, neutron star surface
  - ✓ Optically thin thermal emission : thermal bremsstrahlung + collisionally excited line.
    - ➢ Accretion-powered: Proto-star, Cataclysmic variable, Galaxy, Galaxy cluster
    - ➢ Explosion: Supernova remnant, Normal star

Astrophysical Optically Thin thermal Plasma

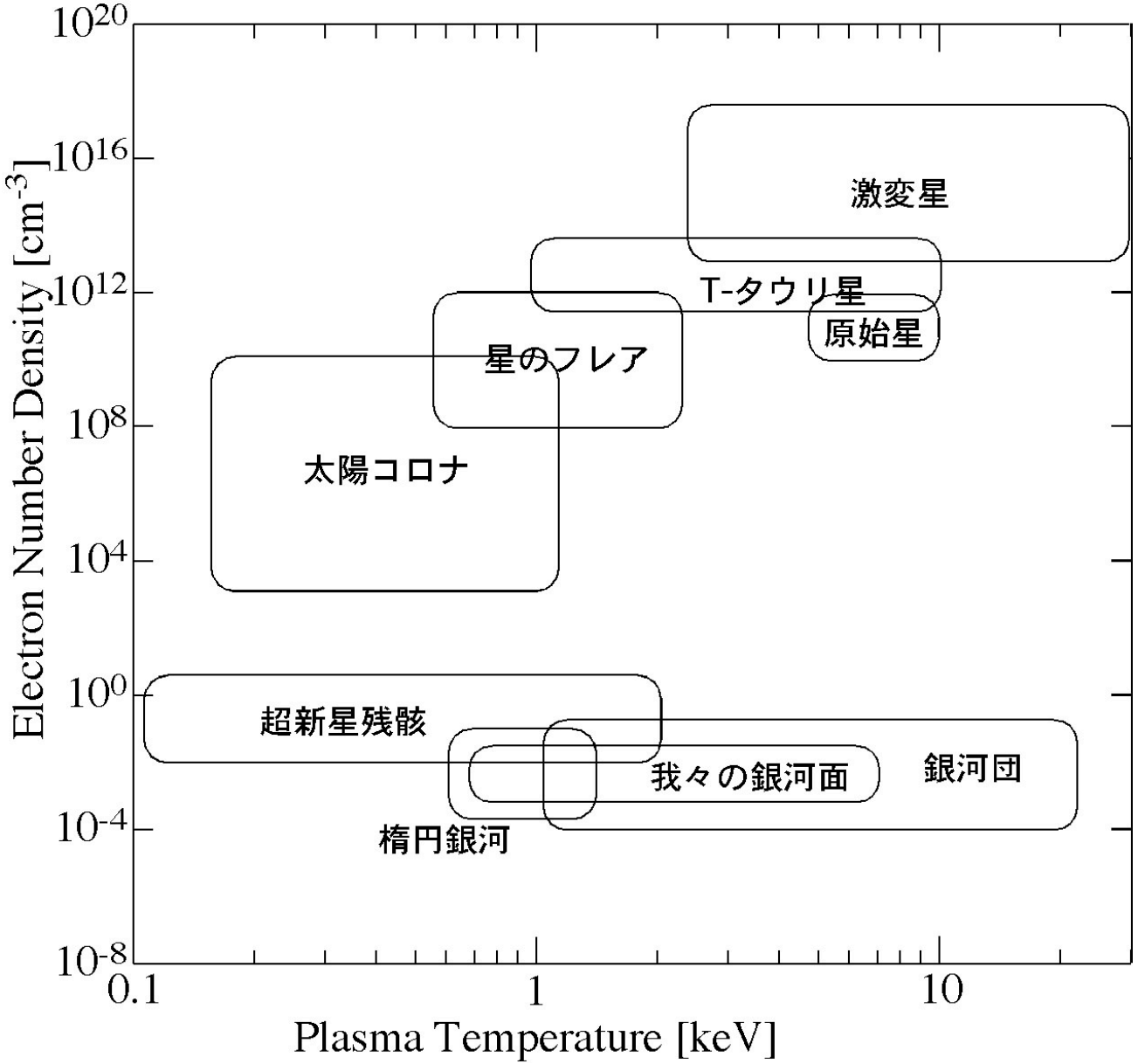

Coronal approximation

1. プラズマは光学的に薄いため、放射はプラズマによって減衰せず、原子のエネルギー準位の分布にも影響を与えない。
2. ガスの密度は充分に低く、原子の励起状態の存在確率は基底状態に比べて無視できるほど小さい。
3. 放射によってプラズマから失われるエネルギーはnon-radiativeな力学的な加熱(主として電子による衝突)によって賄われる。
4. プラズマ中の電子とイオンのエネルギー分布は、共通温度*T*のMaxwell分布で記述される(動力学的熱平衡)。
5. 電離分布は定常状態にあり、エネルギーの入出力によって決定されている(電離平衡)。

Calculation of Ionization Distribution

$$\frac{1}{n_e}\frac{dN_{Z,z}}{dt} = N_{Z,z-1}S_{Z,z-1} - N_{Z,z}\left(S_{Z,z} + \alpha_{Z,z}\right) + N_{Z,z+1}\alpha_{Z,z+1}$$

$S_{Z,z}$: ionization rate [cm^3s^{-1}]

- ✓ collisional ionization
- ✓ collisional excitation auto-ionization

$\alpha_{Z,z}$: recombination rate [cm^3s^{-1}]

- ✓ radiative recombination
- ✓ dielectronic recombination

Z: Atomic number, z: ionization degree

- Coronal approximation: =0

$$\frac{N_{Z,z+1}}{N_{Z,z}} = \frac{S_{Z,z}(T)}{\alpha_{Z,z+1}(T)}$$

Ionization Distribution

Arnaud & Rothenflug (1985)
Arnaud & Raymond (1992)

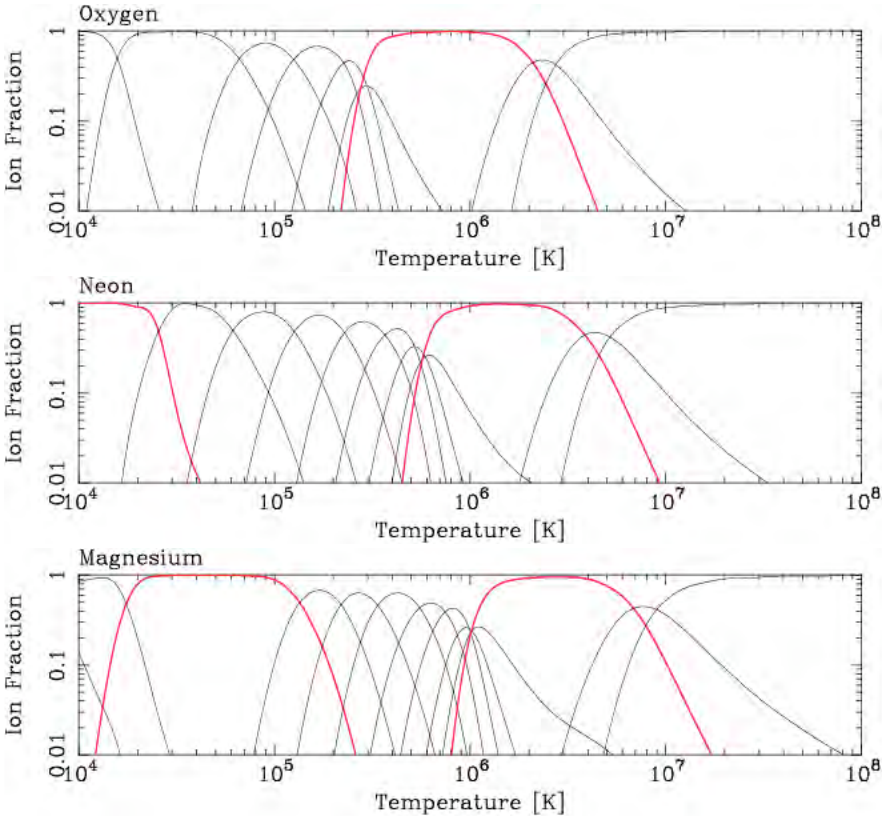

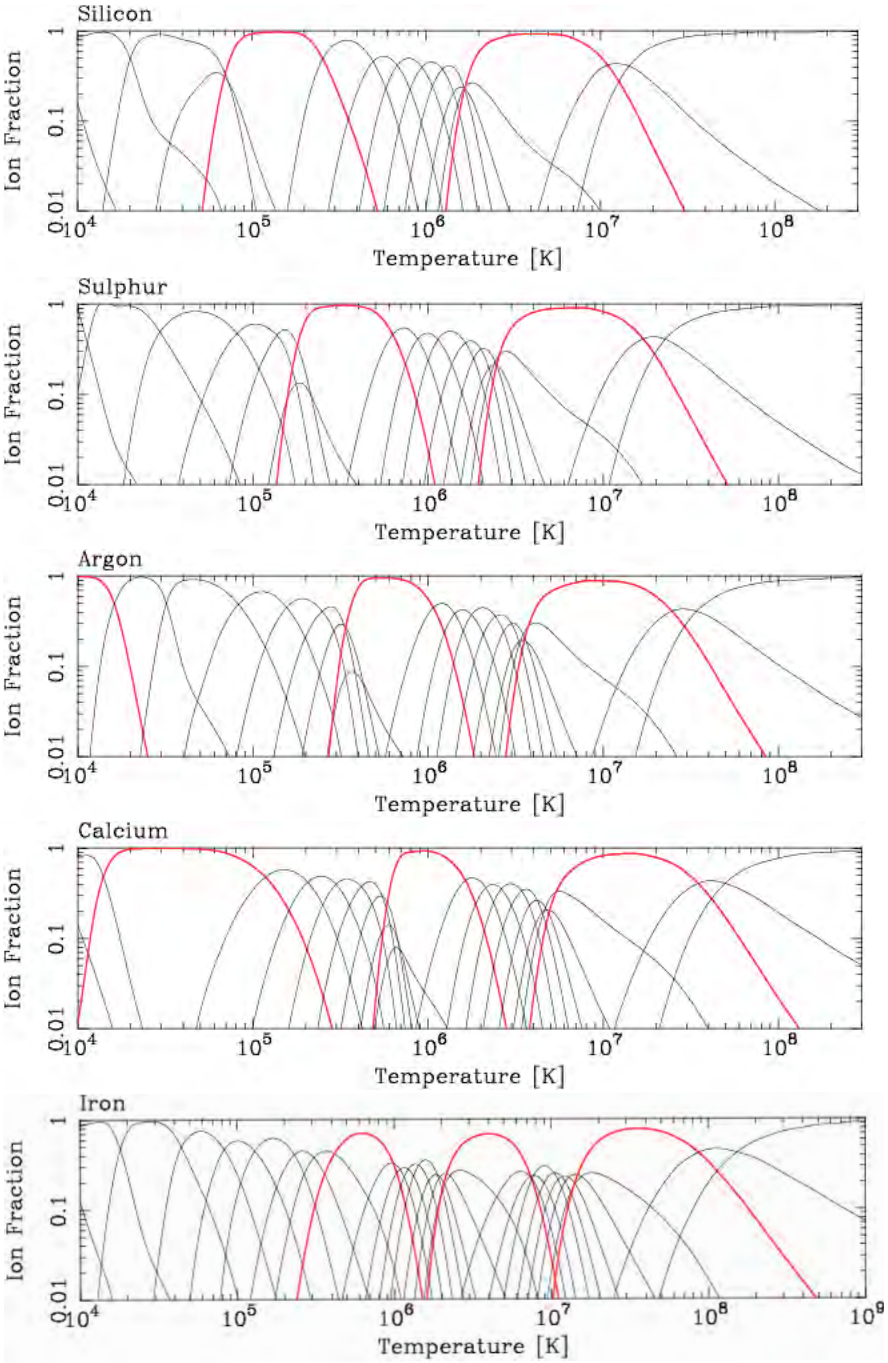

Plasma with T=$10^{6\text{-}8}$K

- Kα lines originating from
  He-like/H-like states
  of O through Fe
- L-shell emission from Fe (>0.7keV)

Typical Spectrum of Cataclysmic Variable

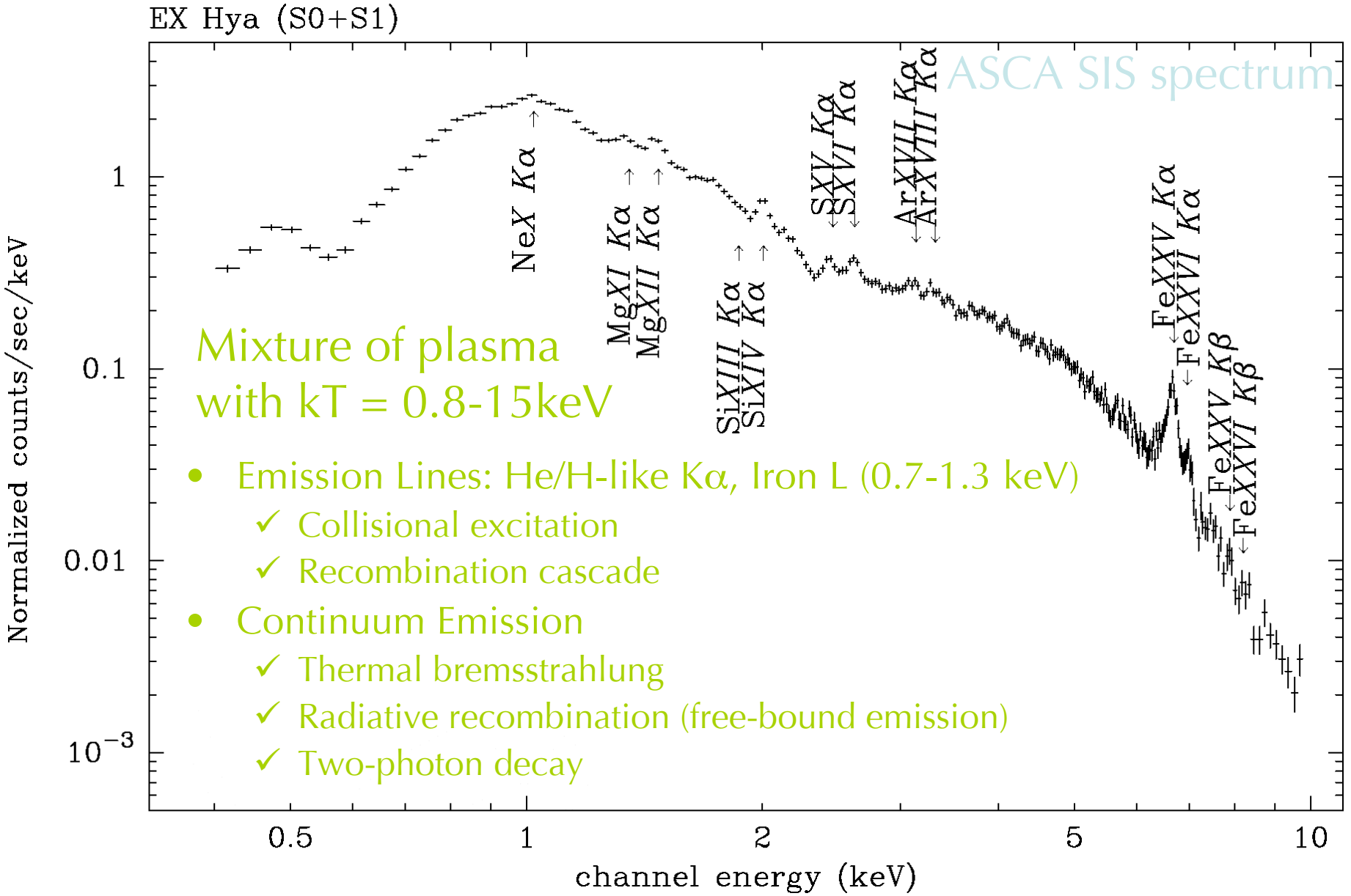

Cataclysmic Variables

- White Dwarf + secondary star ($M < 0.6M_{\odot}$)

  WD: $M \sim M_{\odot} \sim 10^{33}$g, $R \sim R_{E} \sim 10^{9}$cm, $\rho \sim 10^{6}$g/cc

  sustained by the degenerate pressure of electrons
- The secondary filles Roche lobe and mass accretion onto the white dwarf takes place through the innter Lagrangian (L_1) point.

Roche lobe

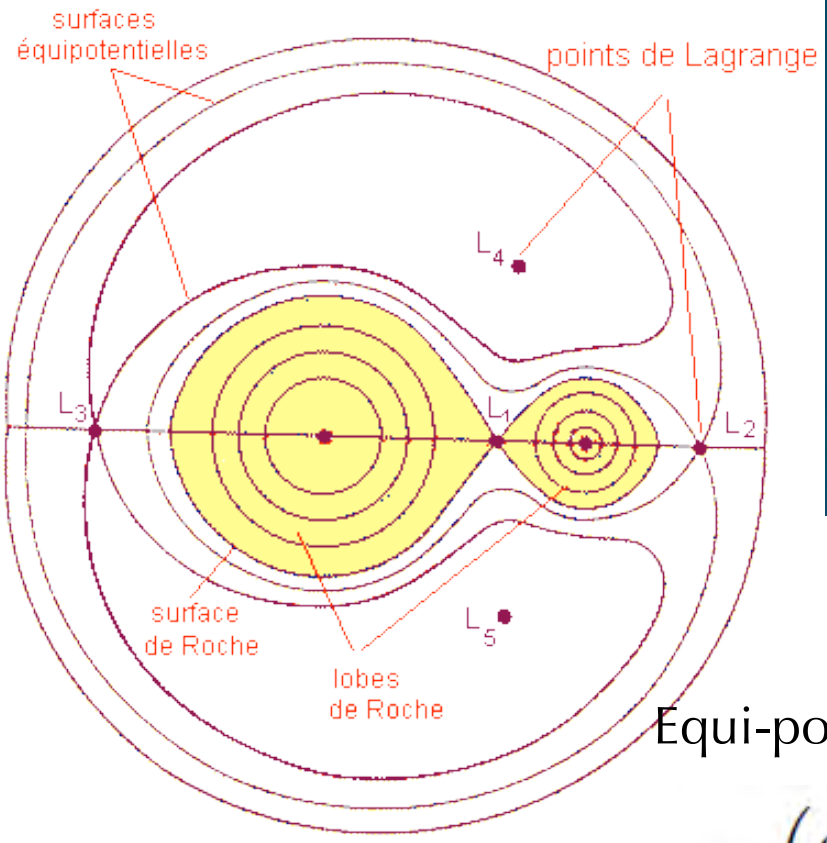

Potentiel de gravitation
dans un système binaire

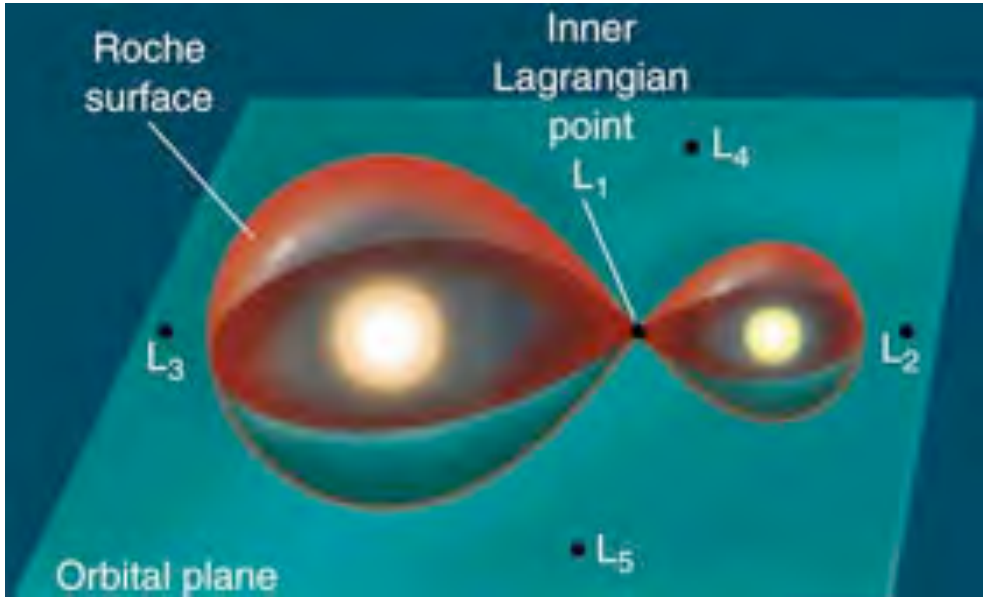

Equi-potential surface on the corotating coordinate

$$m\left(\frac{d^2\boldsymbol{r}}{dt^2}\right)_{\text{rot}} = -m\,\nabla\Phi(\boldsymbol{r}) - 2m\,\boldsymbol{\omega}\times\left(\frac{d\boldsymbol{r}}{dt}\right)_{\text{rot}}$$

$$\Phi(\boldsymbol{r}) = -\frac{GM_1}{|\boldsymbol{r}-\boldsymbol{r}_1|} - \frac{GM_2}{|\boldsymbol{r}-\boldsymbol{r}_2|} - \left(\frac{1}{2}\boldsymbol{\omega}\times\boldsymbol{r}\right)^2$$

Radiation from CVs

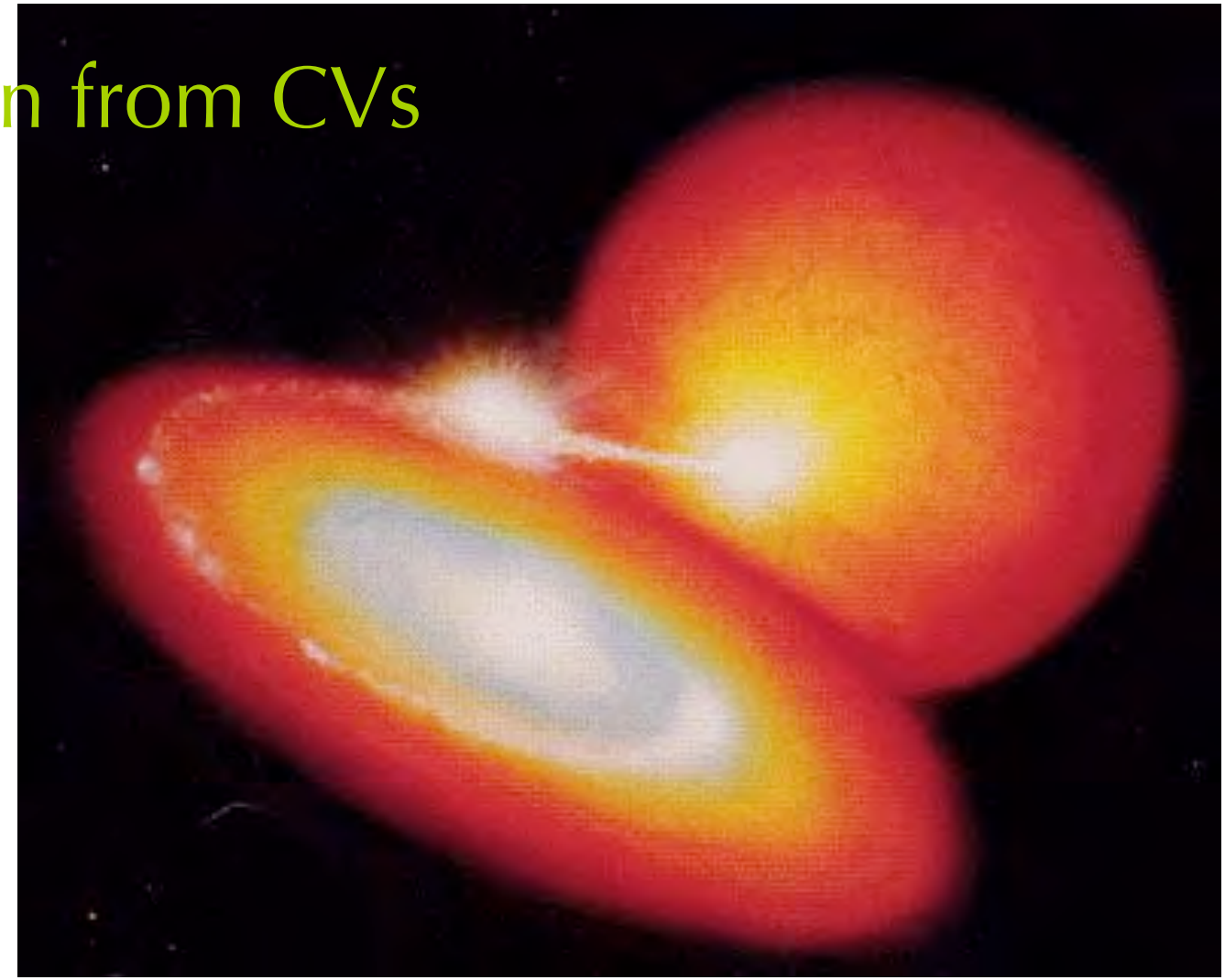

- Infrared : Secondary star (T < 4000K)
- Optical/UV : Standard accretion disk
- X-ray : Boundary layer, Accretion column

Standard Accretion Disk

- Optically thick/Geometrically thin ($h << r$).
- Quasi-Keplerian rotation ($v_r << v_\phi$).
- Frictional heat locally released via blackbody radiation.

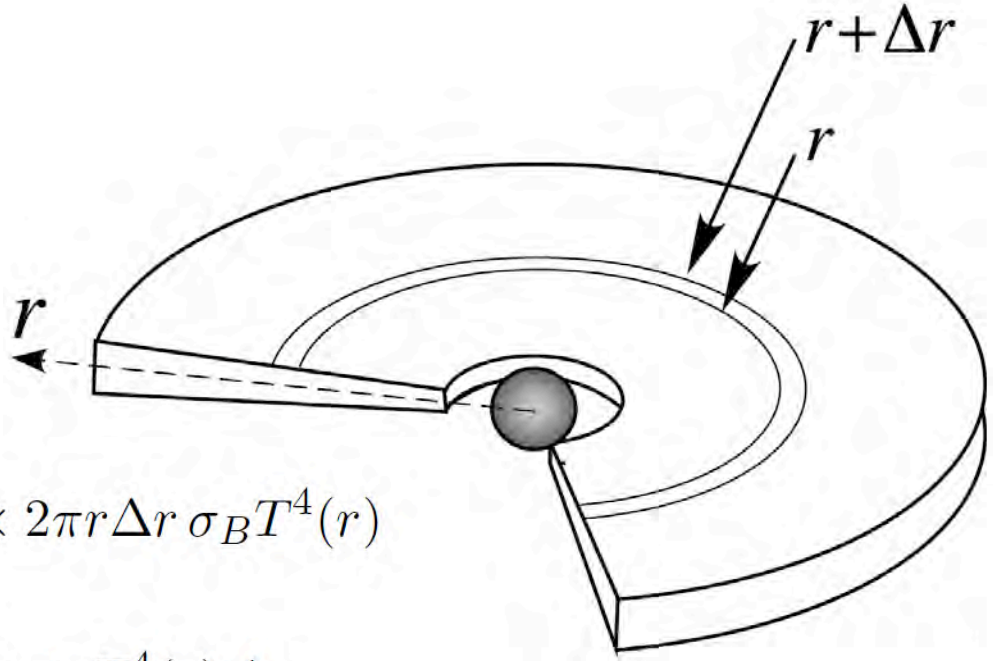

$$\frac{1}{2}\left[-\frac{GM\dot{M}}{r+\Delta r}-\left(-\frac{GM\dot{M}}{r}\right)\right] = 2\times 2\pi r\Delta r\,\sigma_B T^4(r)$$

$$\frac{GM\dot{M}}{2r^2}\Delta r = 4\pi r\,\sigma_B T^4(r)\,\Delta r$$

$$\therefore\ T(r) = \left[\frac{GM\dot{M}}{8\pi r^3\sigma_B}\right]^{1/4} \propto r^{-3/4}$$

典型的には
$T(R_*)$ ~10^5K

Hard X-ray Emission from non-magnetic CVs

- Standard accretion disc (T_{in}~10^5 K)
- The rotation speed of WD at its surface is usually much smaller than $v_K(R_*)$ (~5000km/s).

  →For settling down onto the white dwarf, accreting matter is decelerated from v_K to v_* by converting its Keplerian kinetic energy into heat.
- Hard X-ray: Boundary Layer plasma with T~10^8 K.

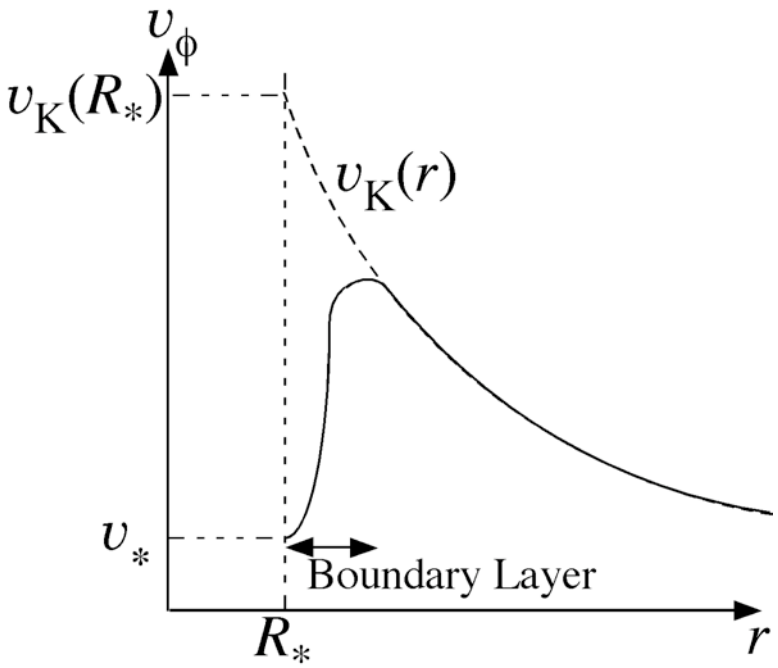

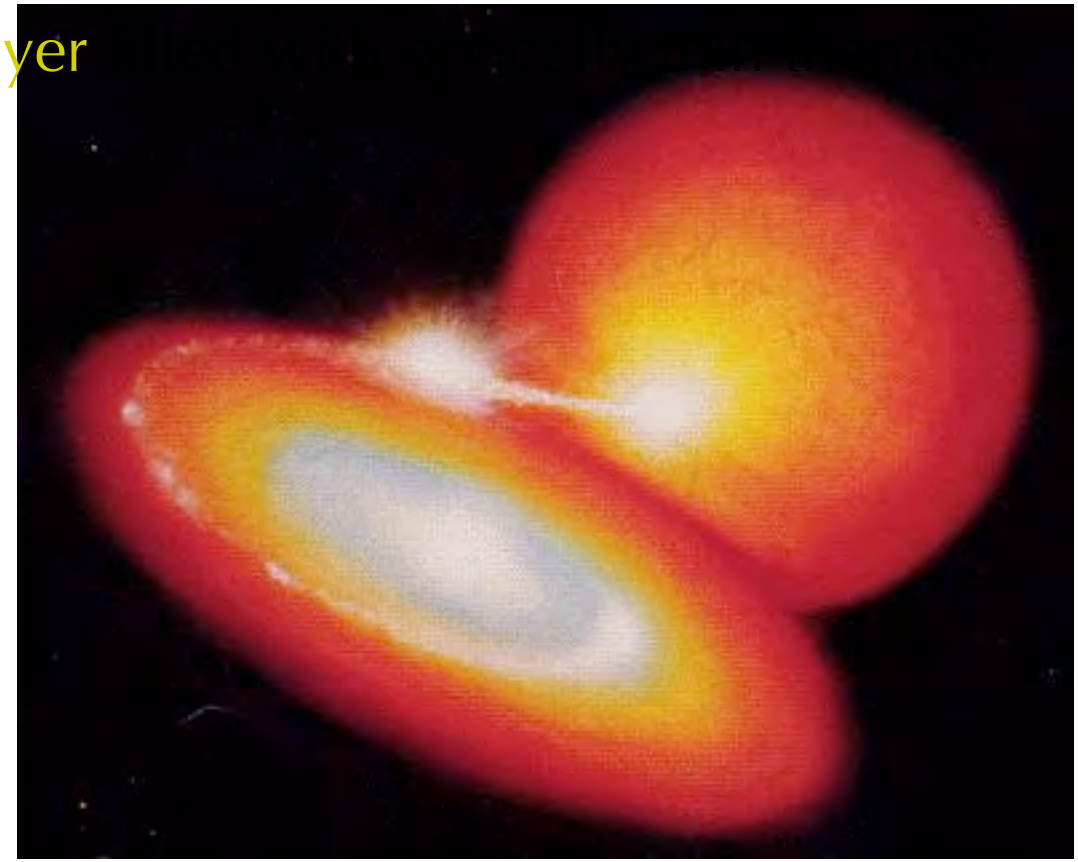

Dwarf Nova Outburst

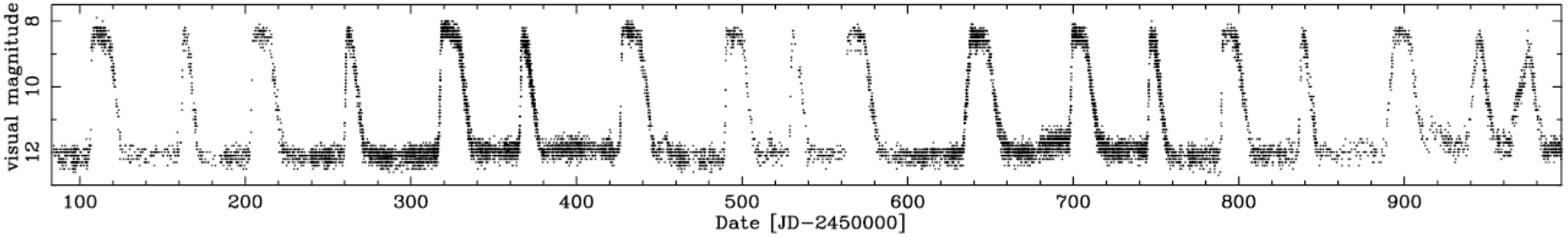

SS Cyg (Weatley et al. 2003)

- DNe outburst is associated with bi-stability of the standard accretion disc (whether H is ionized or not : (Osaki 1996).
- Close to the boundary layer: free-free emissivity (dominating the cooling process in T >10^7K) ~n^2

⇨ Cooling and heating are both catastrophic whenever one dominates over the other.

⇨ M-dot < 10^{16}g/s: optically thin.

⇨ M-dot > 10^{16}g/s: optically thick.

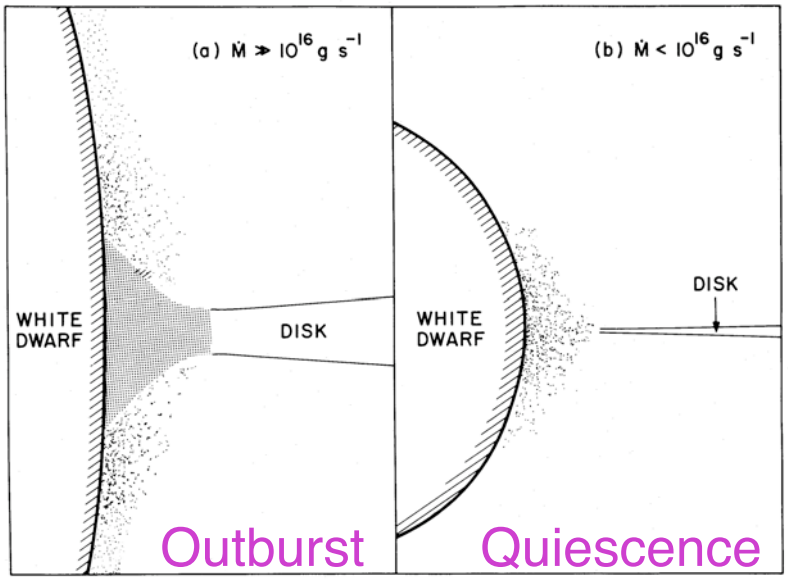

Patterson & Raymond (1985)

DN outburst of SS Cyg

Wheatley et al. (2003)

- Multi-waveband observation in 1996 Oct.
  - ➢AAVSO: Outer accretion disc
  - ➢EUVE: Innter accretion disc
  - ➢RXTE: Boundary Layer (2-15keV).
- Optically thin to thick transition of BL is clearly detected for the first time.
- BL physics is qualitatively confirmed.

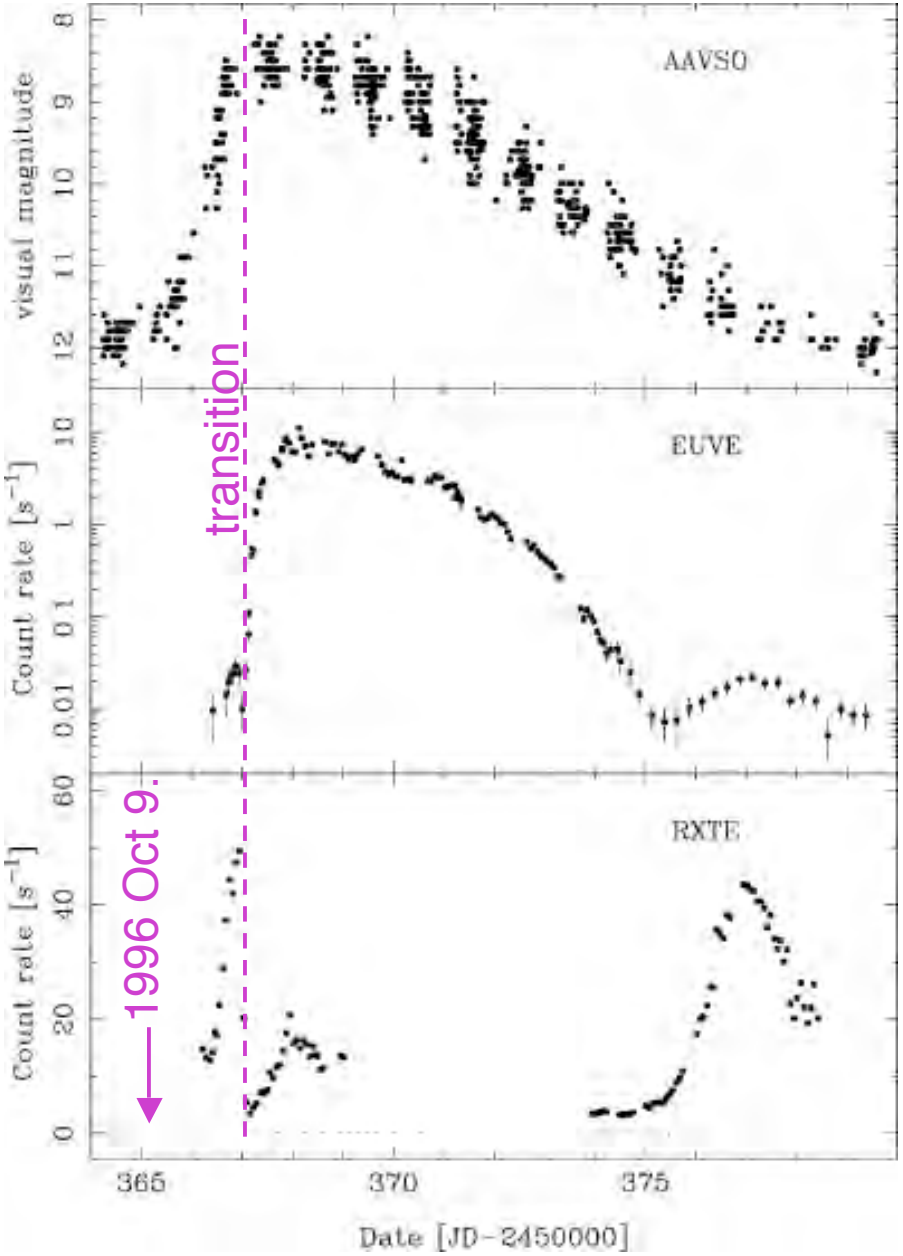

Physics of the Boundary Layer

- Detail of BL is still unknown, such as;
  - r_{BL}: the outer radius of BL.
  - θ_{BL}: the opening angle of BL.
    - ✓ Complete thermalization at r_{BL}: 3-dimentional.
    - ✓ Optically thin ADAF: rather close to 2-dimensional.
  - their variation as a function of M-dot.
    - ✓ In the classical picture, BL is optically thick during the outburst, then,

Where does hard X-ray in outburst originate ?

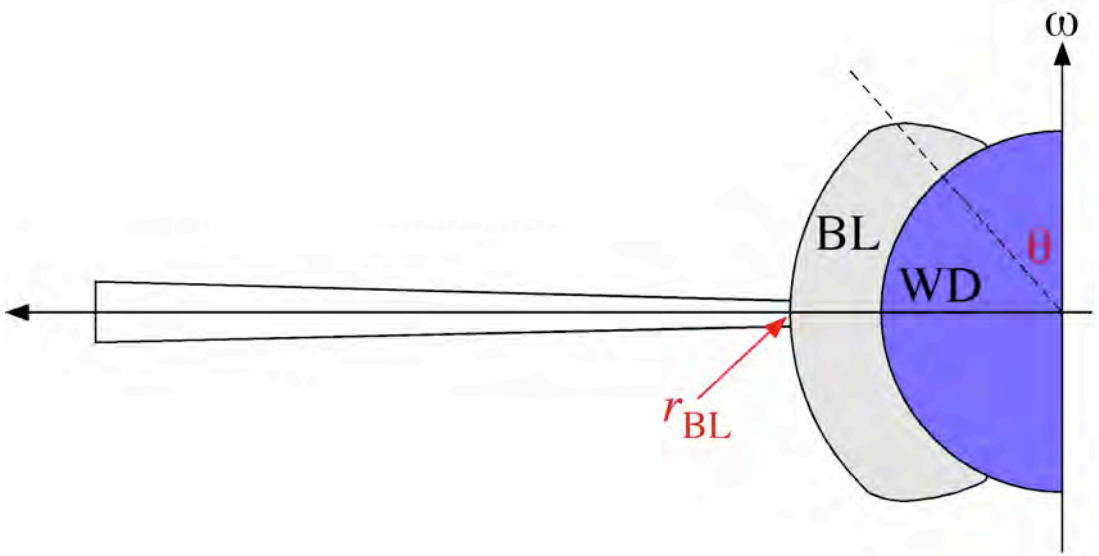

Suzaku Observation of SS Cyg

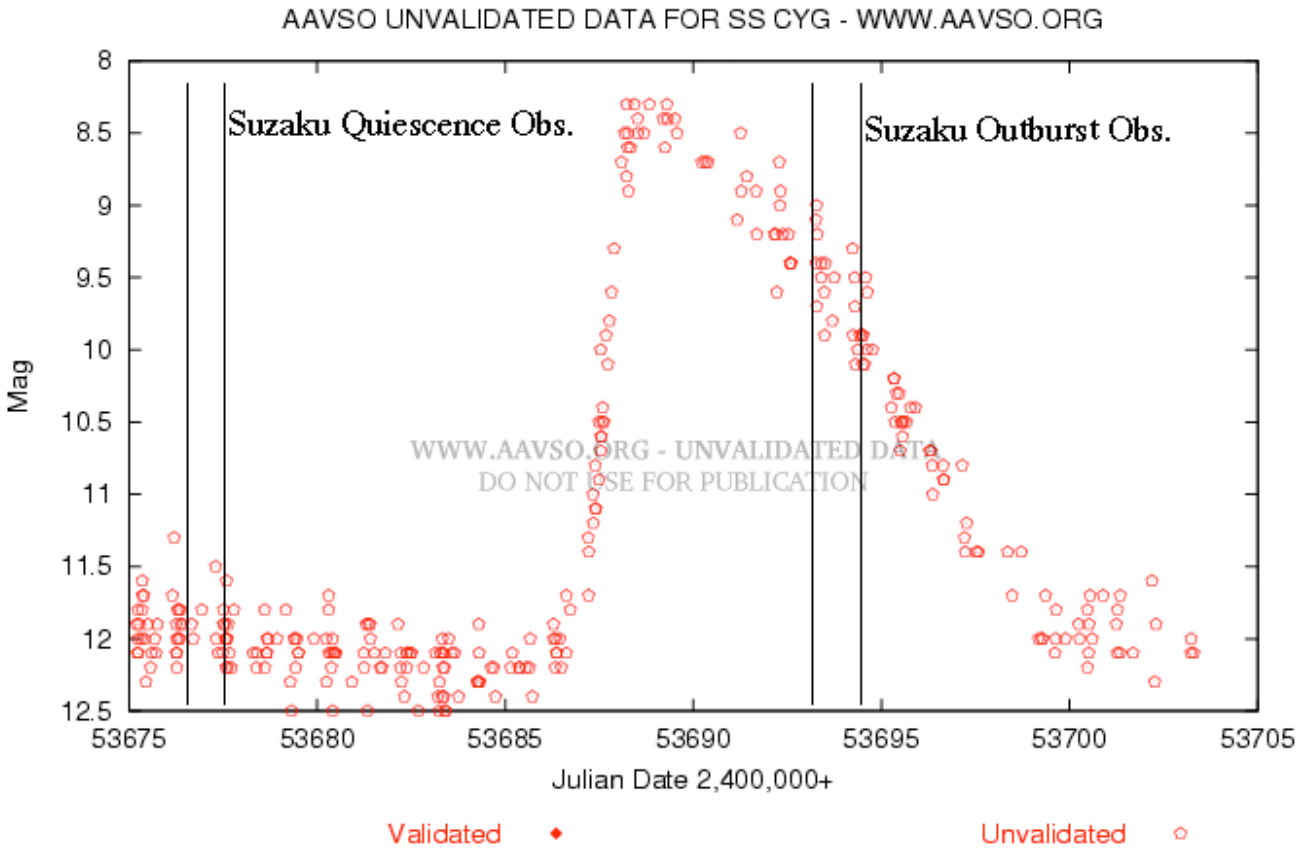

- The brightest DN, system parameters are known very well.
  $D = 166\text{pc}, M_1 = 1.19M_\odot/M_2 = 0.70M_\odot, i \sim 50\text{deg}$
- Observation in Quiescence: 2005 Nov. 2 40ksec
- Observation in Outburst (ToO): 2005 Nov.18 60ksec

CCD Spectra

- $I_Q > I_O$ ($E > 0.3$keV)
- Emission lines from N to Fe.
- T_O~0.2keV, T_{Fe}~10keV

Spectra can be fit with the cooling flow model:

$kT_{min} = 0.1$ keV
kT_{max} ~33 keV(Q)
~10 keV(O)
$Z_{Fe} = 0.54\ Z_\odot$

- Soft blackbody emission

in $E < 0.3$keV in Outburst.
⇨$L_{disk} = 4\pi r_{BL}^2\ \sigma_B T_{in}^4$
⇨T_{in}, M-dot, r_{BL} although calibration is still insufficient in this band.

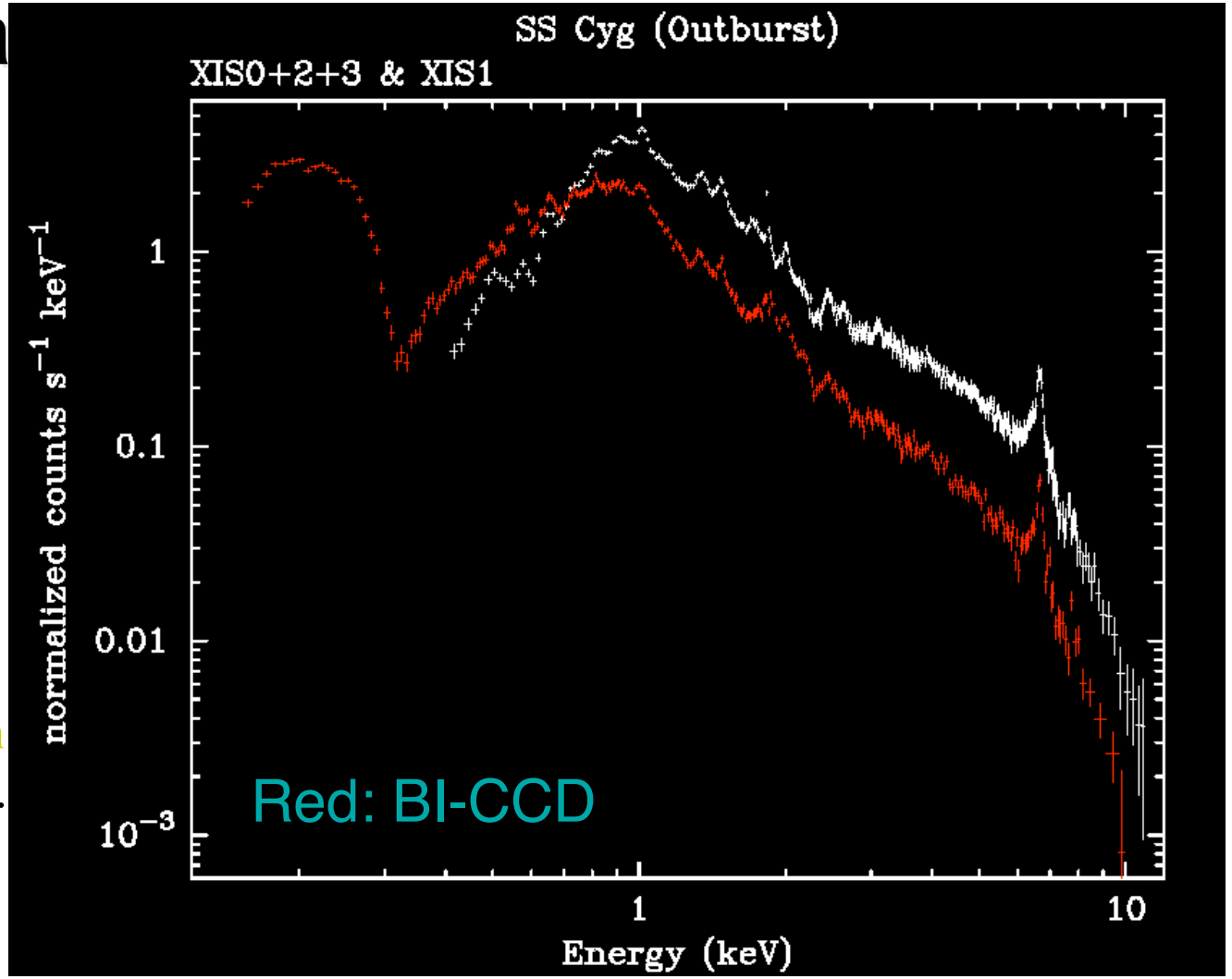

Fluorescent Fe K_α line

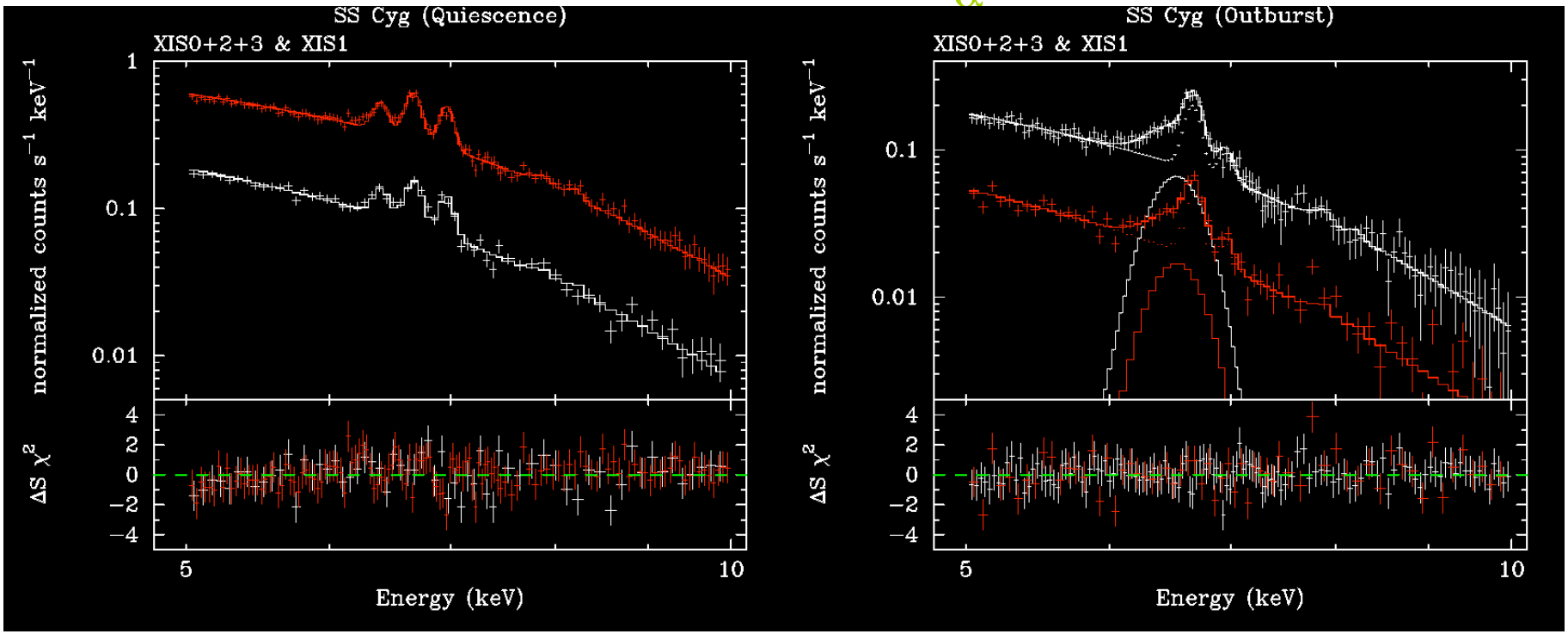

- Narrow (WD) and broad (v~1000km/s from disc) components.
- Reflection originates both from inner disc and WD surface.
- $EW_{\rm nar}$ ~20eV ($Z_{\rm Fe} = 0.54 Z_\odot$)
  - ⇨ $\Omega_{\rm WD}(r_{\rm BL}) \sim \pi$, hence $r_{\rm BL} \sim 1.2 R_{\rm WD}$
- $EW_{\rm br} / EW_{\rm nar} = \Omega_{\rm disc}(r_{\rm BL}, \theta_{\rm BL}) / \Omega_{\rm WD}(r_{\rm BL})$
  - ⇨ $\theta_{\rm BL}$ can be constrained (need simulation)

- Only broad component is visible, probably broader than in Q.
  - ⇨ Smaller $r_{\rm BL}$
- Reflection originates mainly from inner disc.

Intermediate Polar

- $B = 0.1\text{-}10 \times 10^6$G.
- $P_{\rm spin} < P_{\rm orb}$
- Inner disc is truncated due to strong B field.
- Accretion

$$\frac{1}{2}\rho v^2(r) = \frac{B^2(r)}{8\pi}$$

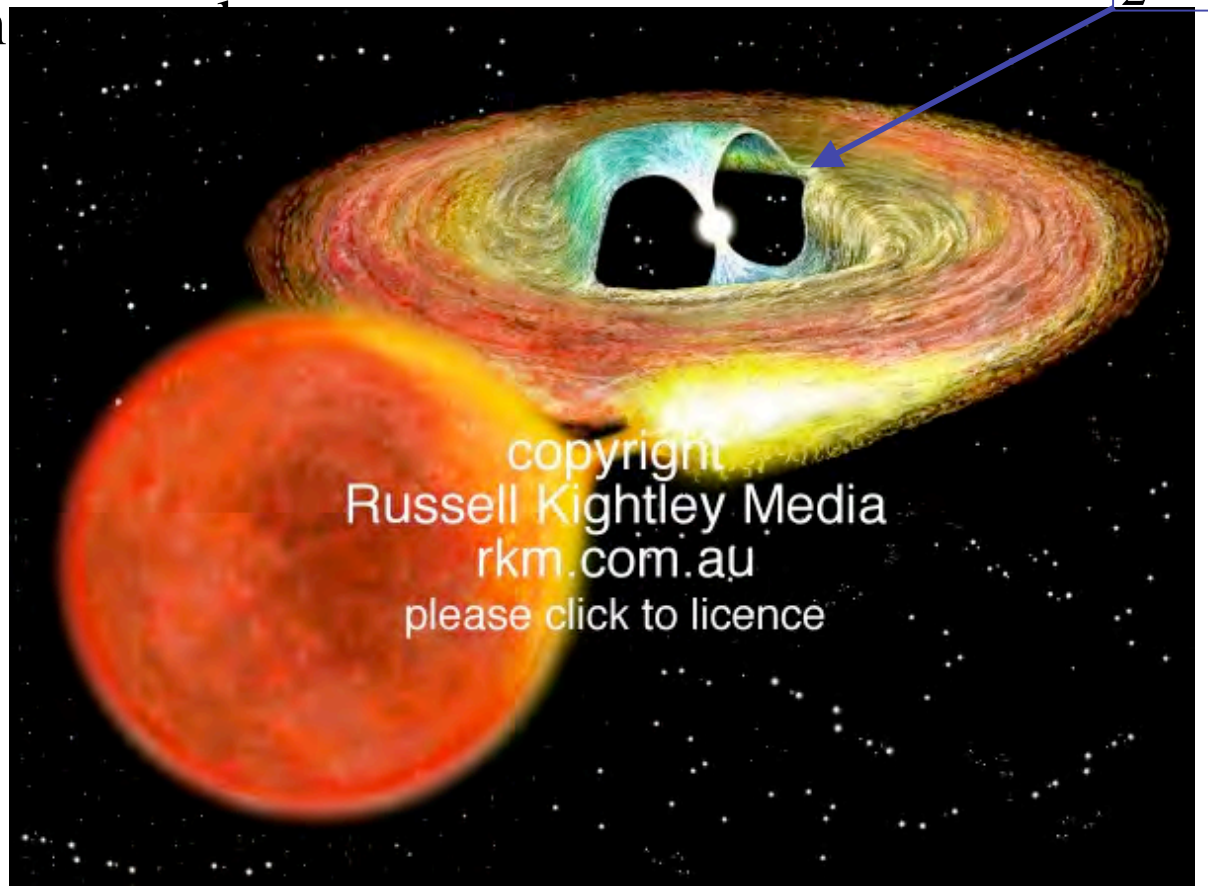

Polar

- B = 10-230 x10^6G
- $P_{spin} = P_{orb}$
- no accretion disc

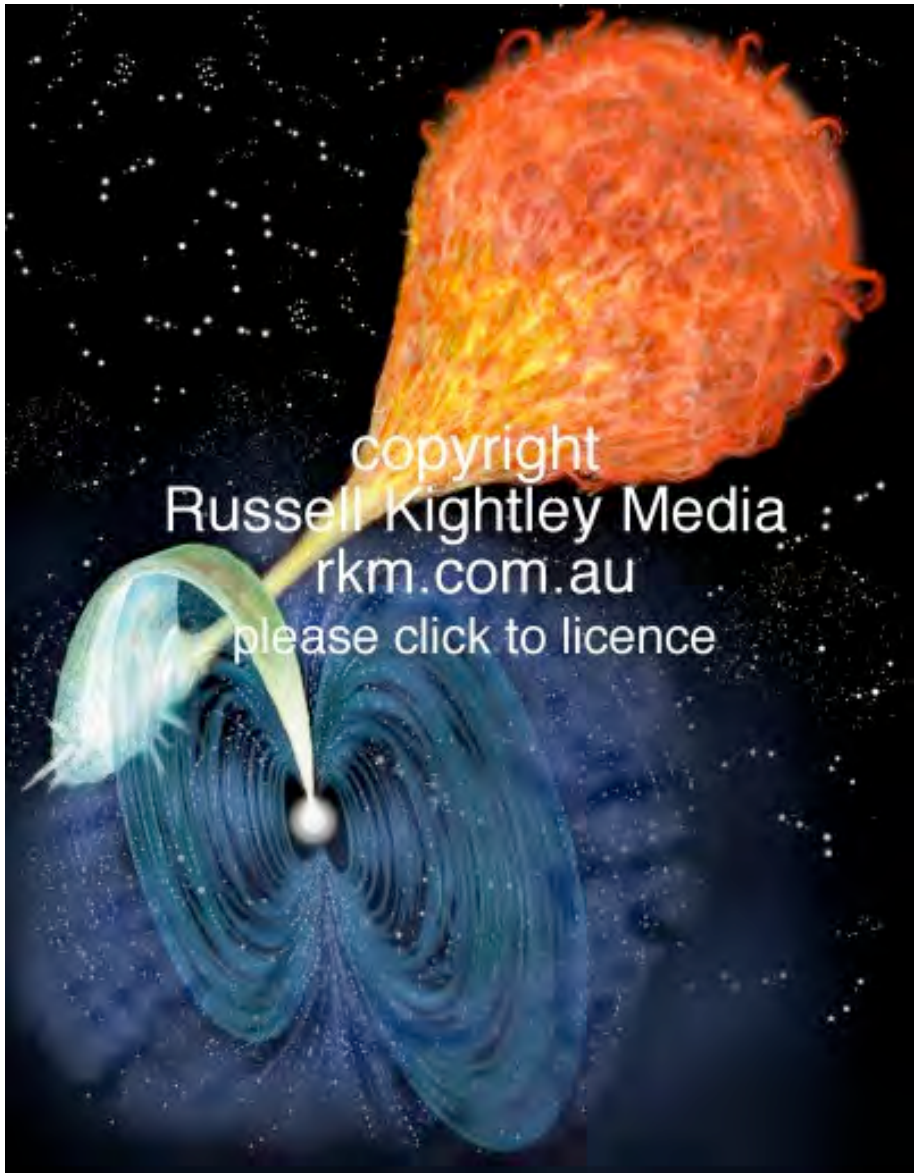

X-ray Emission from Magnetic CV

• Hard X-ray emission occurs from thin thermal plasma due to shock heating ($M \sim 10^2$).

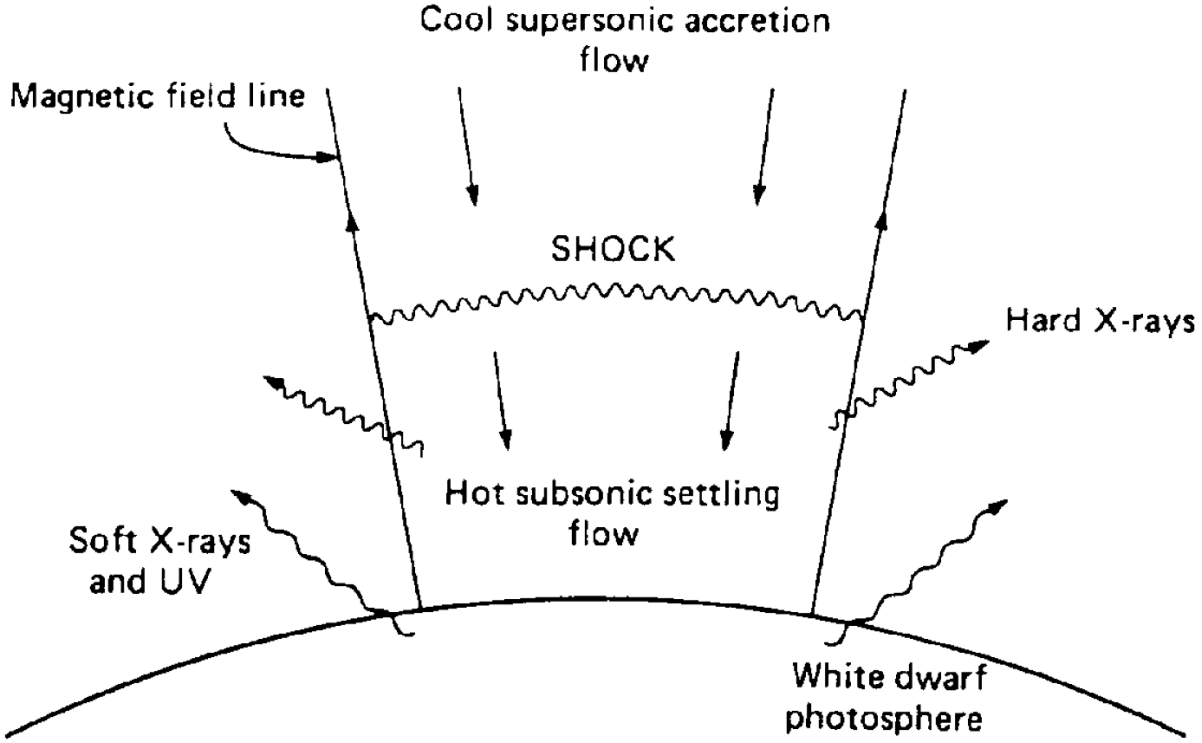

$$kT_S = \frac{3}{8}\frac{GM}{R}\mu m_H = 22\left(\frac{M}{0.6M_\odot}\right)^{4/3} \text{ keV}$$

GK Persei

- P_{spin} = 351s.
- X-ray pulsation at the rotation period of WD.

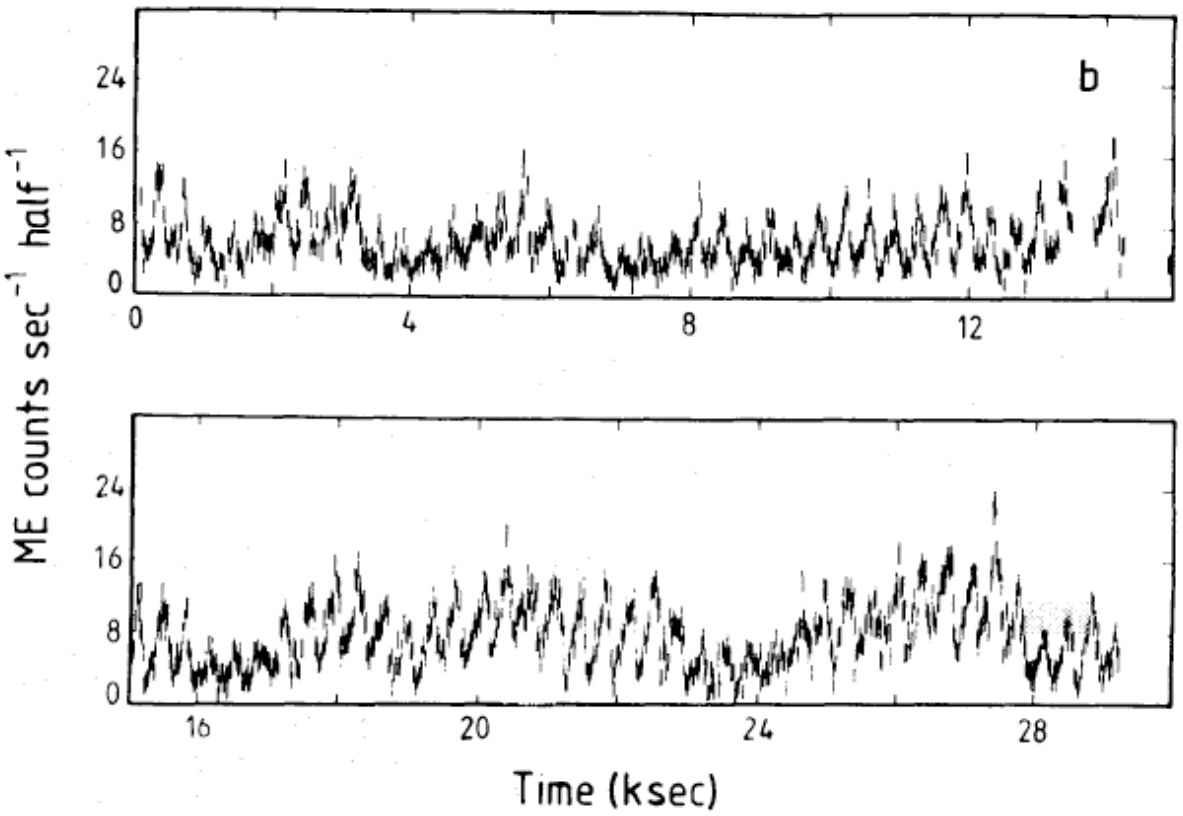

Watson, King, Osborne (1985)

Post-shock accretion flow

- Height of the shock is governed by the cooling (free-free) time scale.
- Typically $h < 0.05 R_{\rm WD}$.
  - ⇨One-dimensional flow.
  - ⇨Gravity change negligible.
- $n_{\rm e} \sim 10^{16\text{-}17}{\rm cm}^{-3}$, $\ell \sim 10^{7}{\rm cm}$

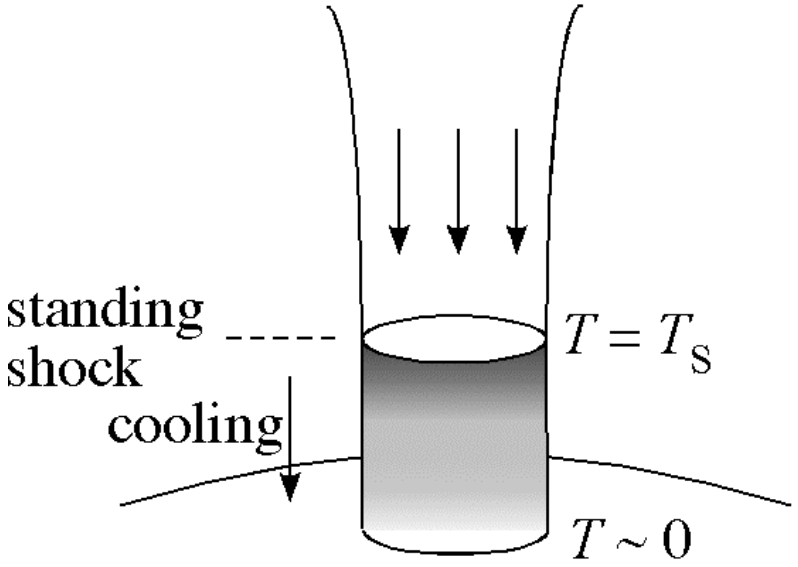

Aizu (1973)

$$\frac{v(z)}{v_{\rm S}} = \frac{T(z)}{T_{\rm S}} = \frac{n_{\rm S}}{n(z)} = \left(\frac{z}{h}\right)^{2/5}$$

Wu et al. (1995)

a: B = 0 MG
b: = 30 MG
c: = 60 MG
d: = 90 MG
Dot m = 1.0 g/cm²/s
M = 0.65$M_\odot$

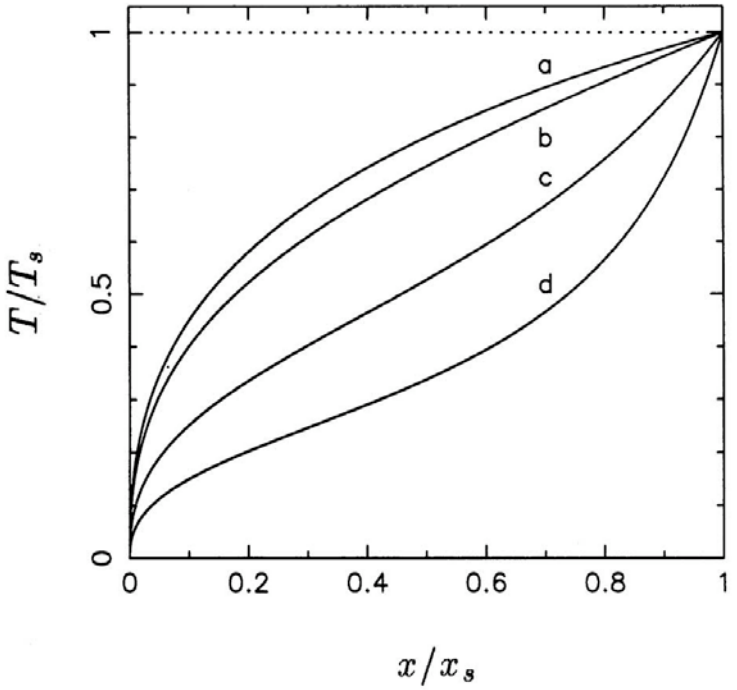

X-ray spectrum of EX Hya

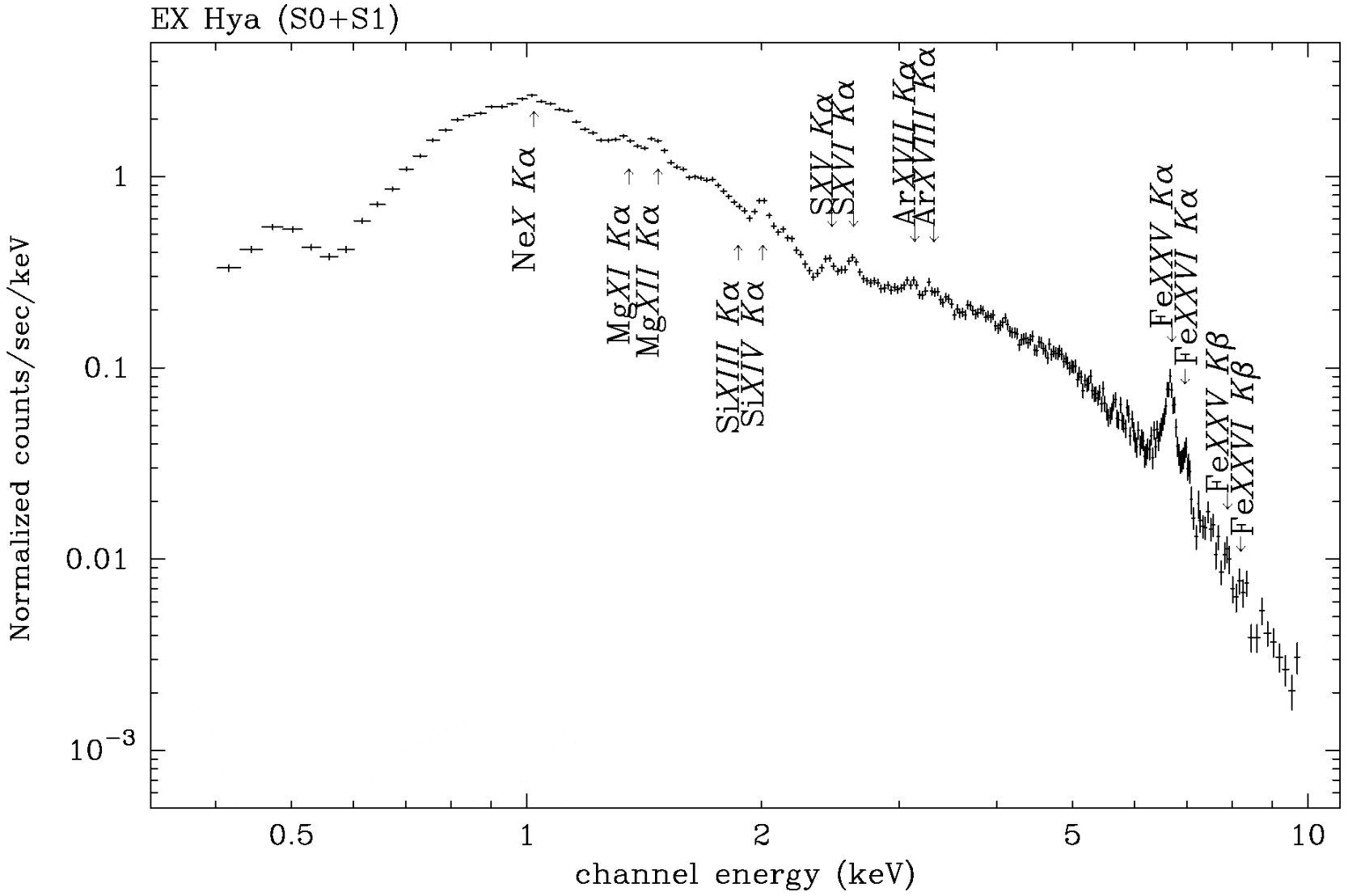

Line Emission Site

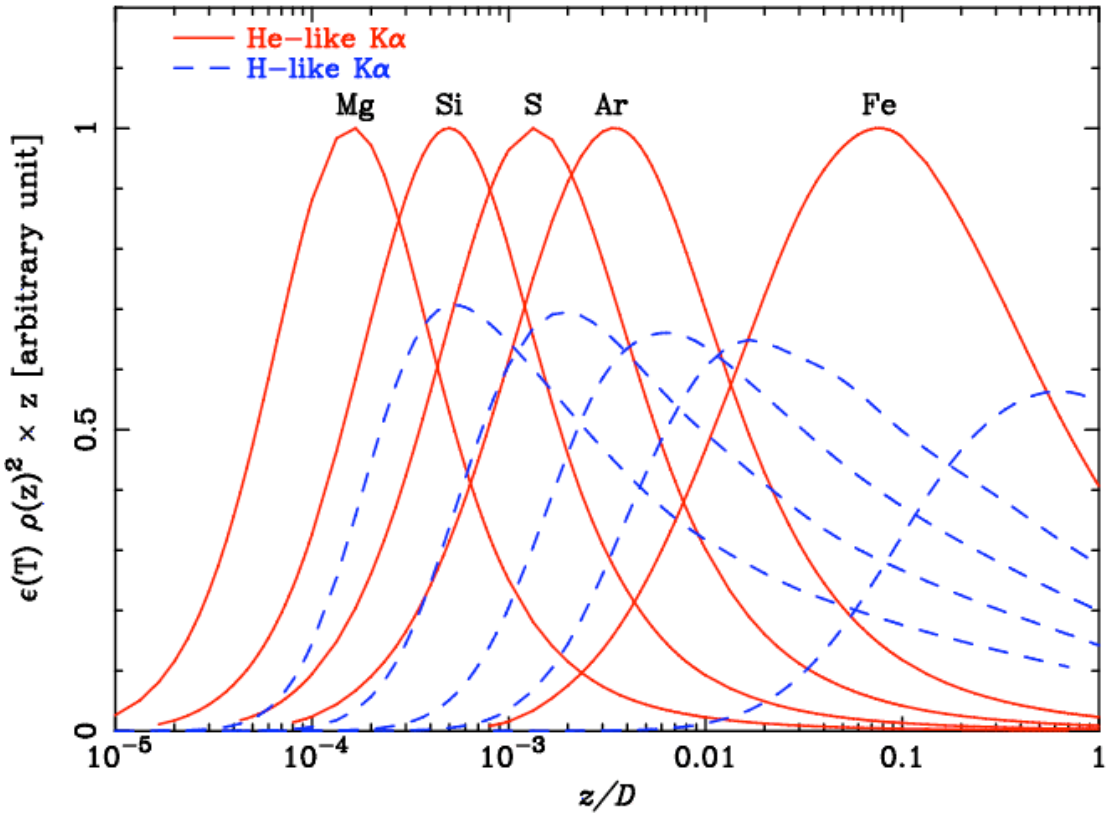

- Iron K_α Line originates from vicinity of the shock.
- The other lines are emitted from the base.

$$\frac{I_{\mathrm{Fe}^{+25}}(T_\mathrm{S},T_\mathrm{B},Z_\mathrm{Fe})}{I_{\mathrm{Fe}^{+26}}(T_\mathrm{S},T_\mathrm{B},Z_\mathrm{Fe})} = R_\mathrm{Fe}(T_\mathrm{S},T_\mathrm{B}), \quad \frac{I_\text{He-like}(T_\mathrm{S},T_\mathrm{B},Z_\text{others})}{I_\text{H-like}(T_\mathrm{S},T_\mathrm{B},Z_\text{others})} = R_\text{others}(T_\mathrm{S},T_\mathrm{B})$$

Mass of the White Dwarf

- EX Hya: $kT_S = 15.4^{+5.3}_{-2.6}$ keV
  With the aid of *M*-*R* relation.

$$R = 7.8\times10^{8}\left[\left(\frac{1.44M_{\odot}}{M}\right)^{2/3} - \left(\frac{M}{1.44M_{\odot}}\right)^{2/3}\right]^{1/2} \text{ [cm]}$$

Naeunberg (1972)

⇨ $M = 0.48^{+0.10}_{-0.06}M_{\odot}$

Fujimoto, Ishida (1997)

- Other White Dwarfs

Ishida, Fujimoto (1999)

- Many small mass WDs in mCV ?

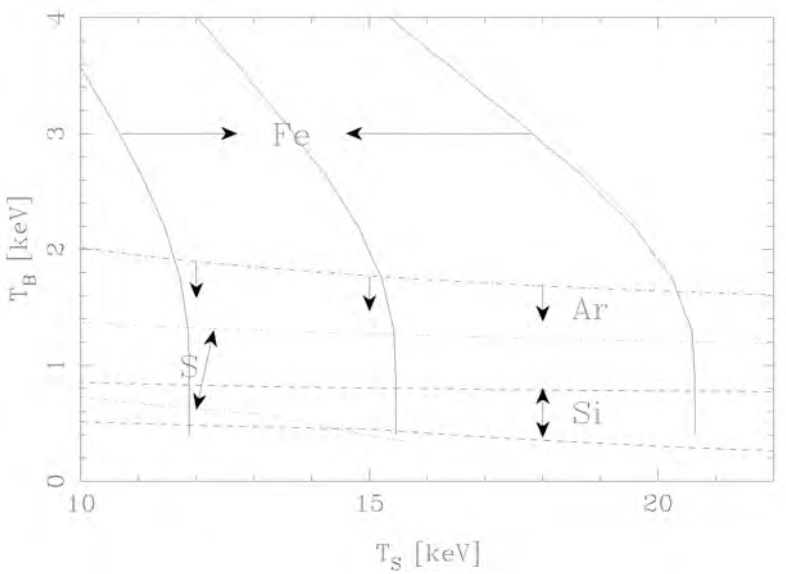

Table. 2 Mass of the White Dwarfs

Target	Mass $[M_{\odot}]$	
	This work	Cropper
EX Hya	$0.48^{+0.10}_{-0.06}$	$0.52^{+0.08}_{-0.12}$
V1223 Sgr	> 0.84	—
RX1712	$0.68^{+0.42}_{-0.26}$	—
AO Psc	$0.40^{+0.13}_{-0.10}$	< 0.80
RXJ0558	> 0.54	—
FO Aqr	> 0.44	> 1.00
TV Col	$0.51^{+0.41}_{-0.22}$	> 0.95
TX Col	$0.66^{+0.73}_{-0.42}$	$0.55^{+0.09}_{-0.11}$
GK Per	$0.52^{+0.34}_{-0.16}$	—

AE Aquarii

- Intermediate Polar (DQ Her) type magnetic CV
- WD + K3-5V *(Welsh et al. 1995)* or K3IV *(Skidmore et al. 2003)*
- $P_{\mathrm{Spin}} = 33.08$ s ($\omega = 0.35$), $P_{\mathrm{Orb}} = 9.88$ h *(Patterson (1979)*
- $M_{\mathrm{WD}} = 0.79\mathrm{M}_{\odot}$, $M_2 = 0.50\mathrm{M}_{\odot}$, $i = 58\pm6$ *(Casares et al. 1996)*
- $D = 102$ pc *(Friedjung 1997)*

X-ray pulse

ASCA light curve

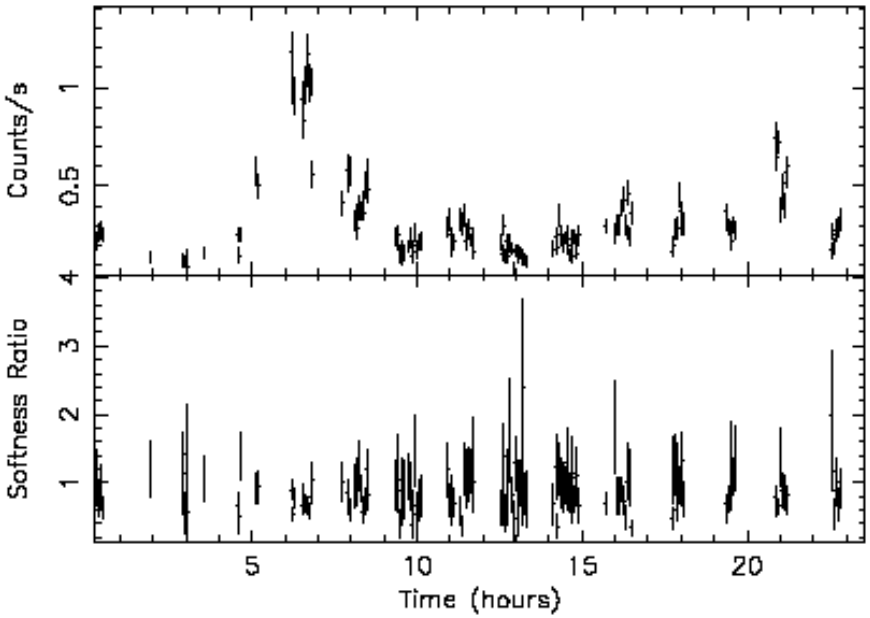

Choi et al. (1999)

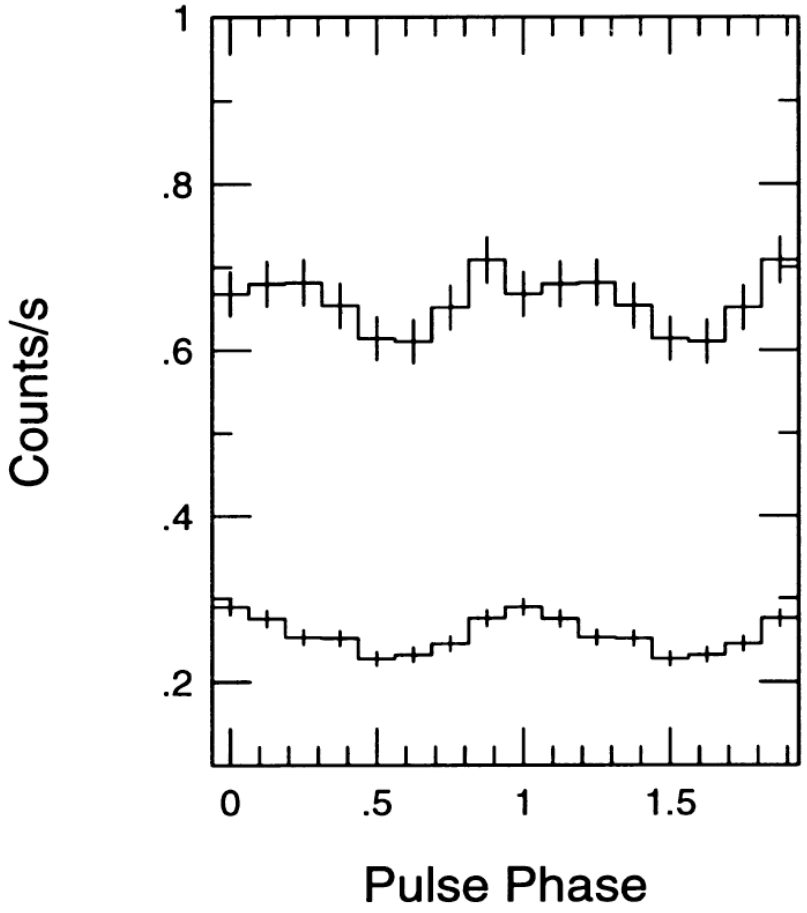

- X-ray pulse at P_{spin}

Average XMM EPIC MOS spectrum

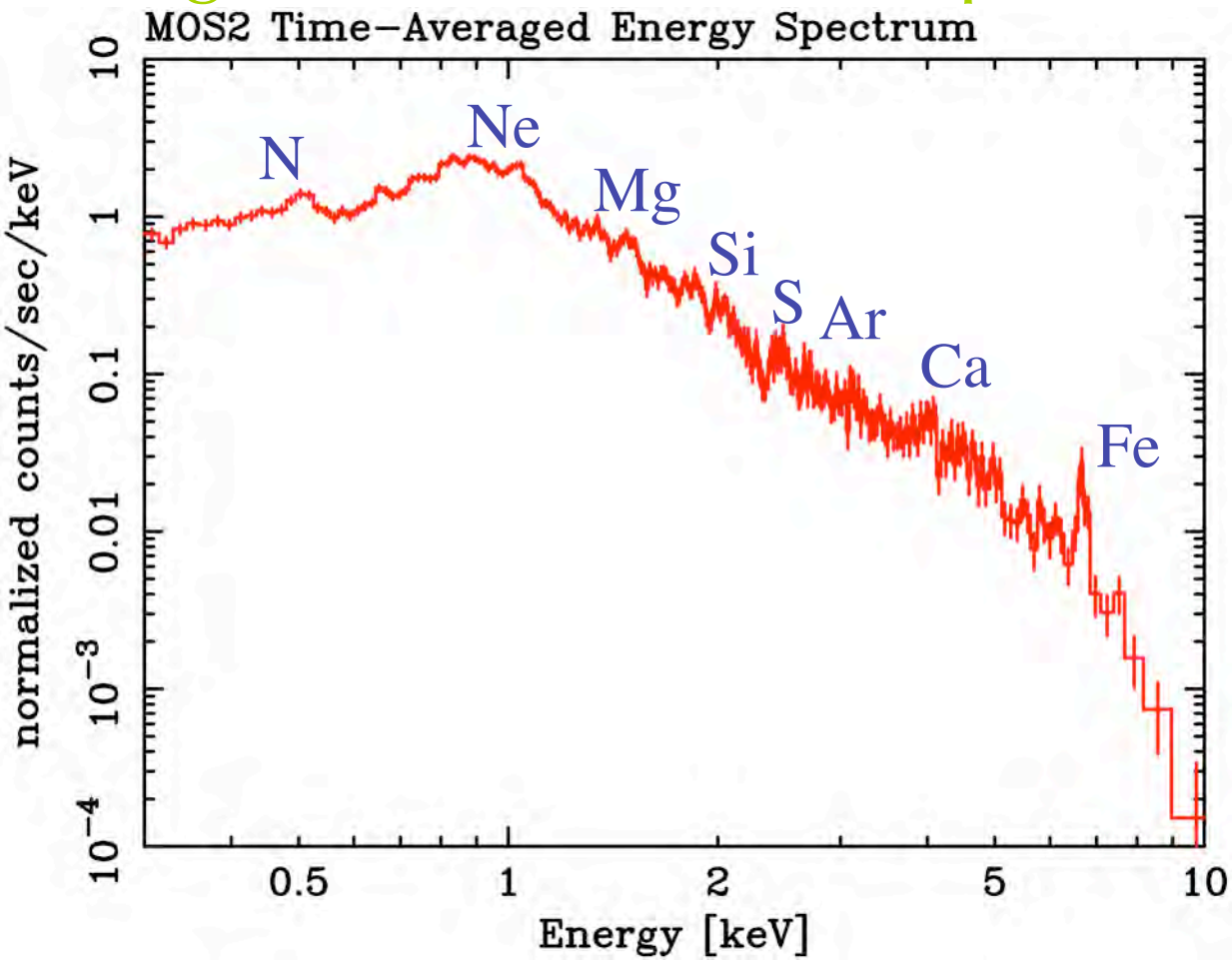

- Multi-T optically thin thermal plasma emission.
- $kT = 0.14, 0.59, 1.21, 4.60$ keV

  (*cf.* kT = 10-40 keV for mCV in general)

Plasma Temperature

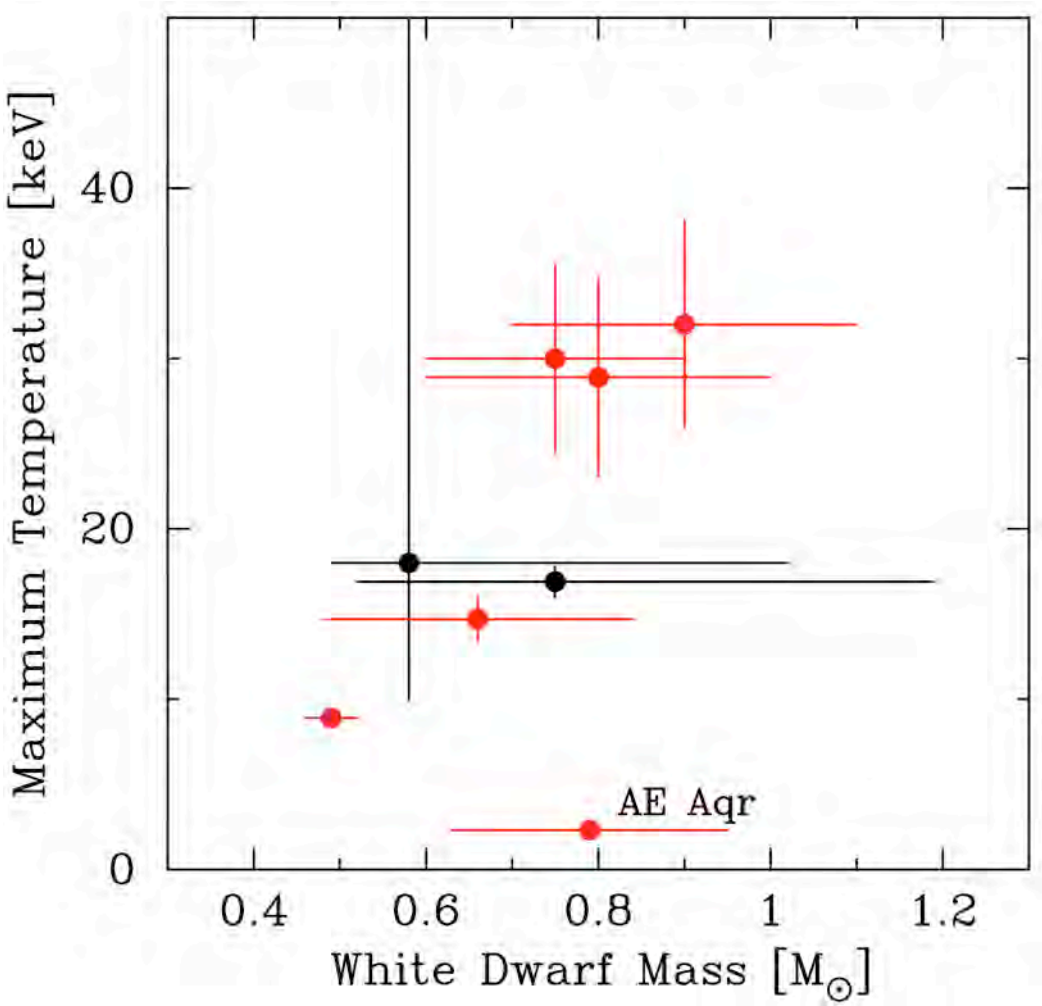

- Really accreting onto WD ?

Spectra from XMM-Newton RGS (E<2keV)

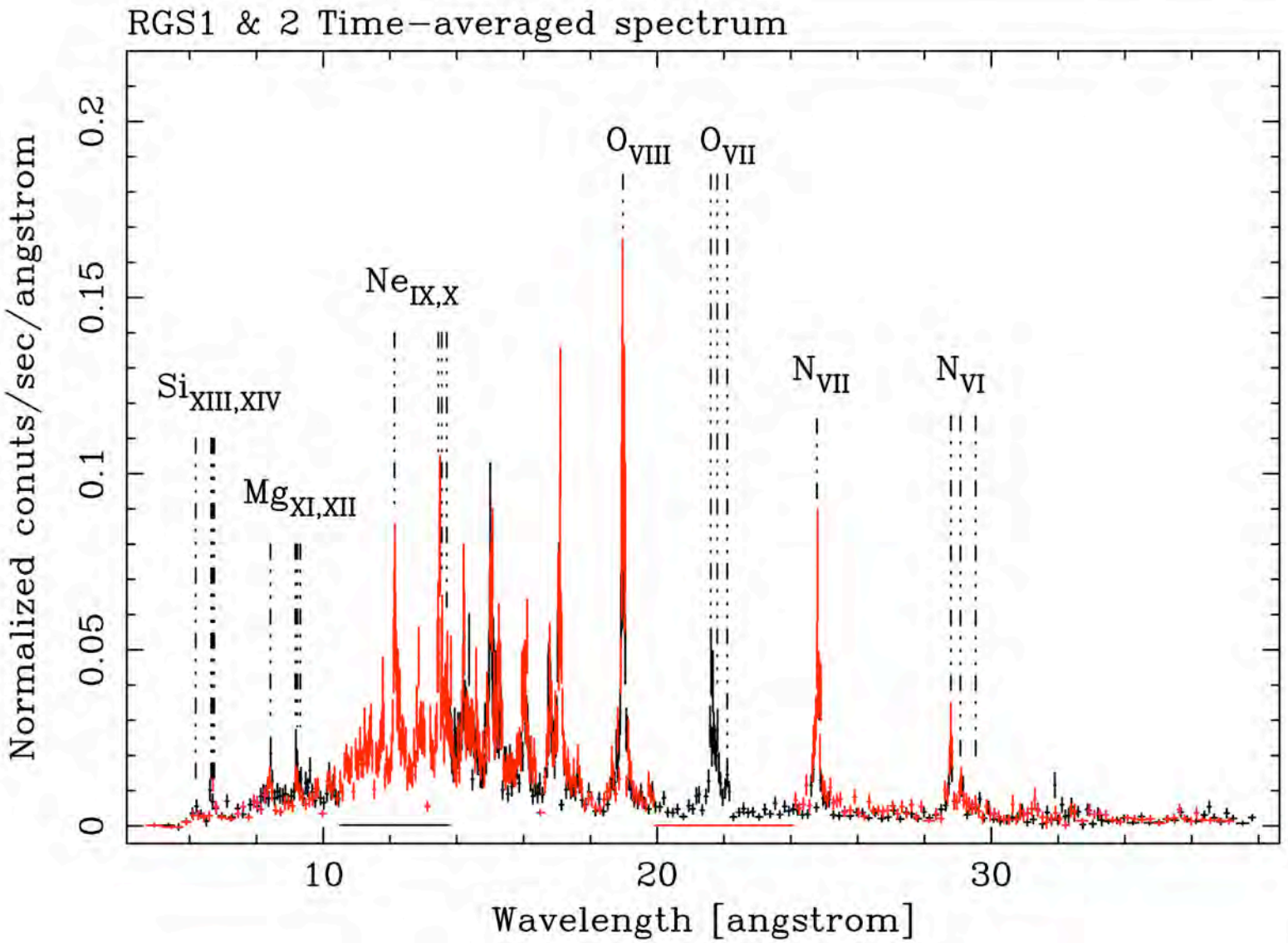

Itoh, Okada, Ishida, Kunieda (2006)

Density from He-like triplet

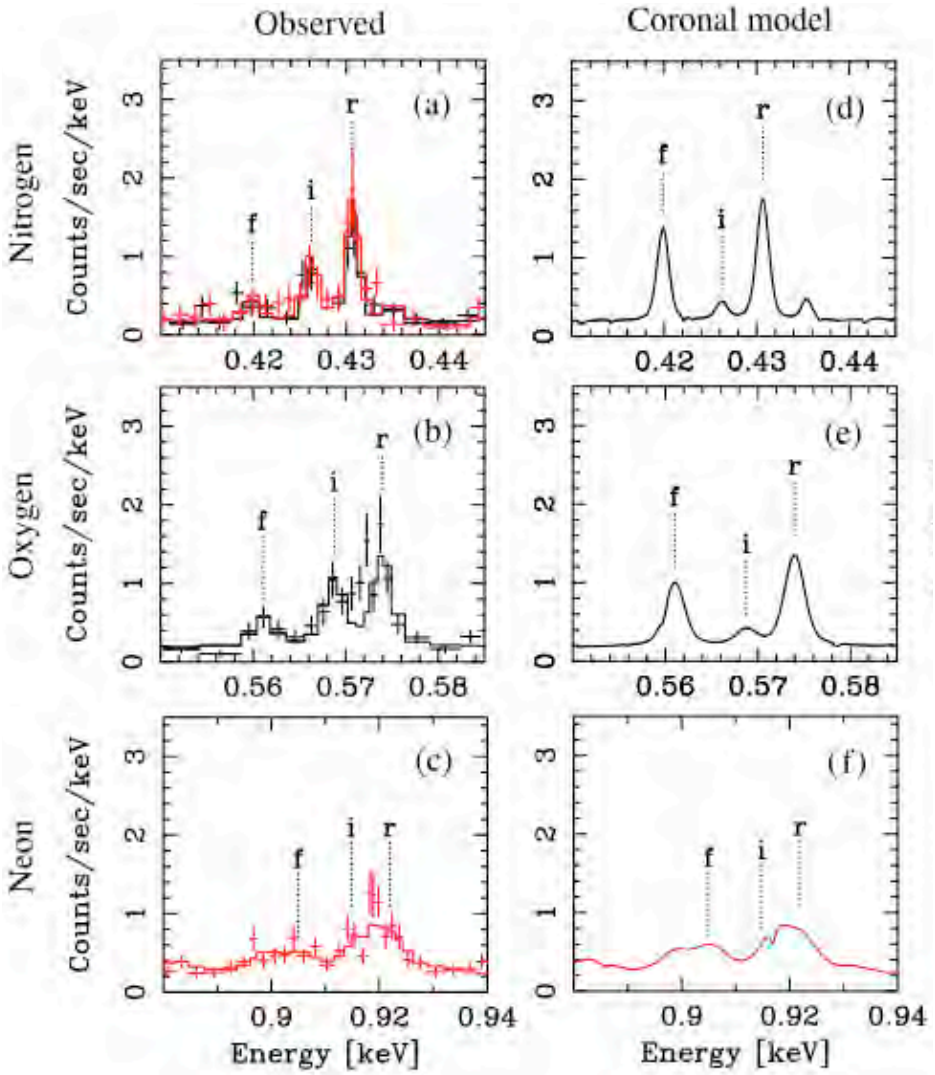

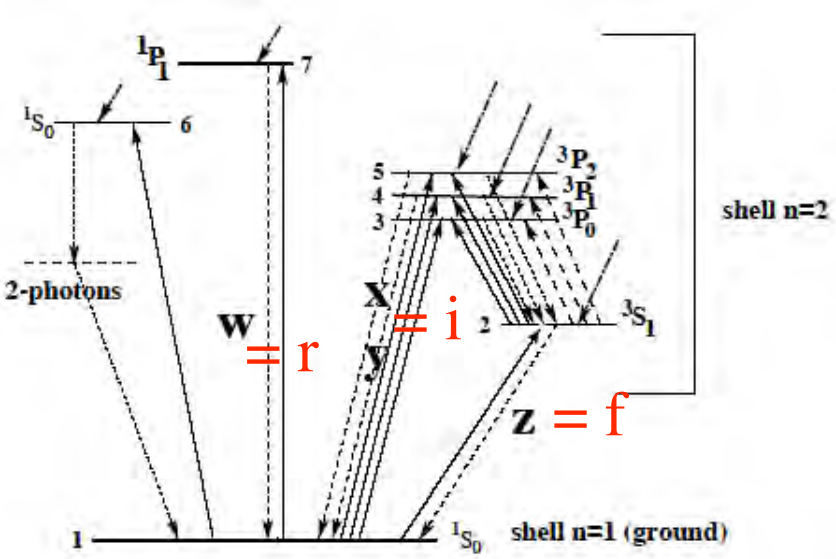

- $^3S_1$ decays through $^3P_{2,1}$ if $A(^3S_1\text{-}^1S_0) \sim n_e C(^3S_1\text{-}^3P_{2,1})$
- Resolving degeneracy between n_e and V in a point source.

Density from He-like triplet

$n_e \sim 10^{11}$ cm^{-3}

$$I_x = f(\mathrm{T}) \int n_e n_{\mathrm{H}}\, \mathrm{dV} = f(\mathrm{T}) \cdot \mathrm{EM}$$

$$V = 10^{31} \sim 10^{32}\ \mathrm{cm}^3$$
$$\ell_p = V^{1/3} = \textbf{2–3 x } 10^{10}\ \textbf{cm}$$

Incompatible with the post-shock polarcap plasma in mCVs

$n_e \sim 10^{16}$ cm^{-3}, $\ell \sim 10^7$ cm

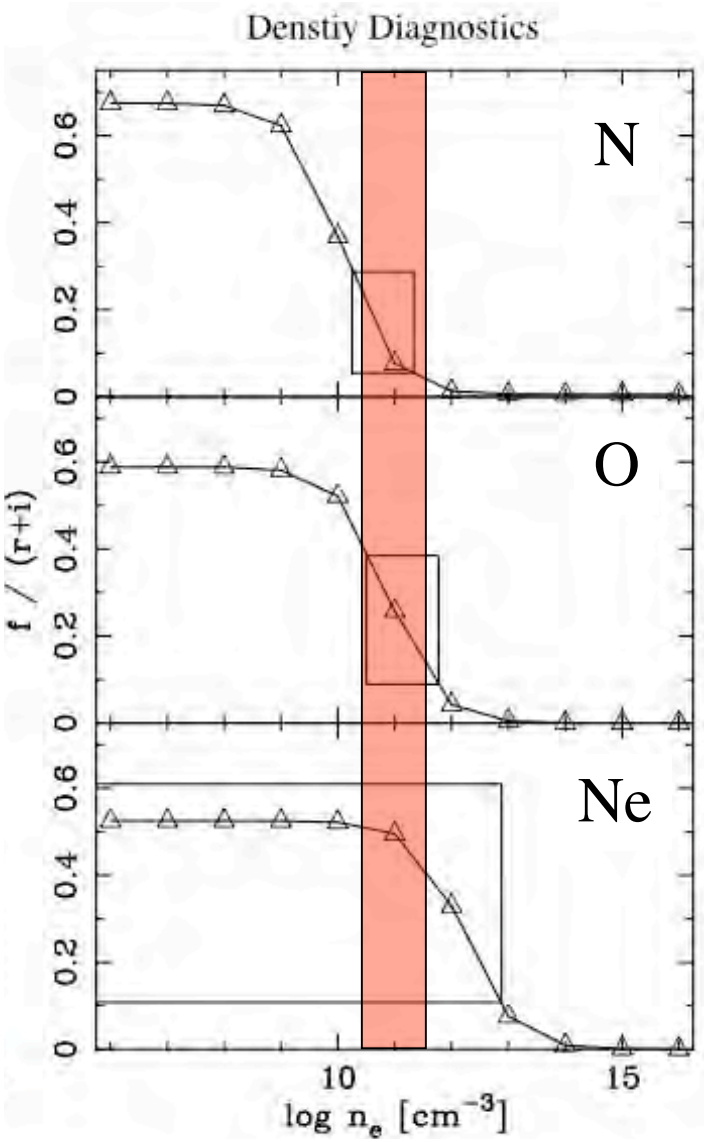

Magnetic Propeller Effect

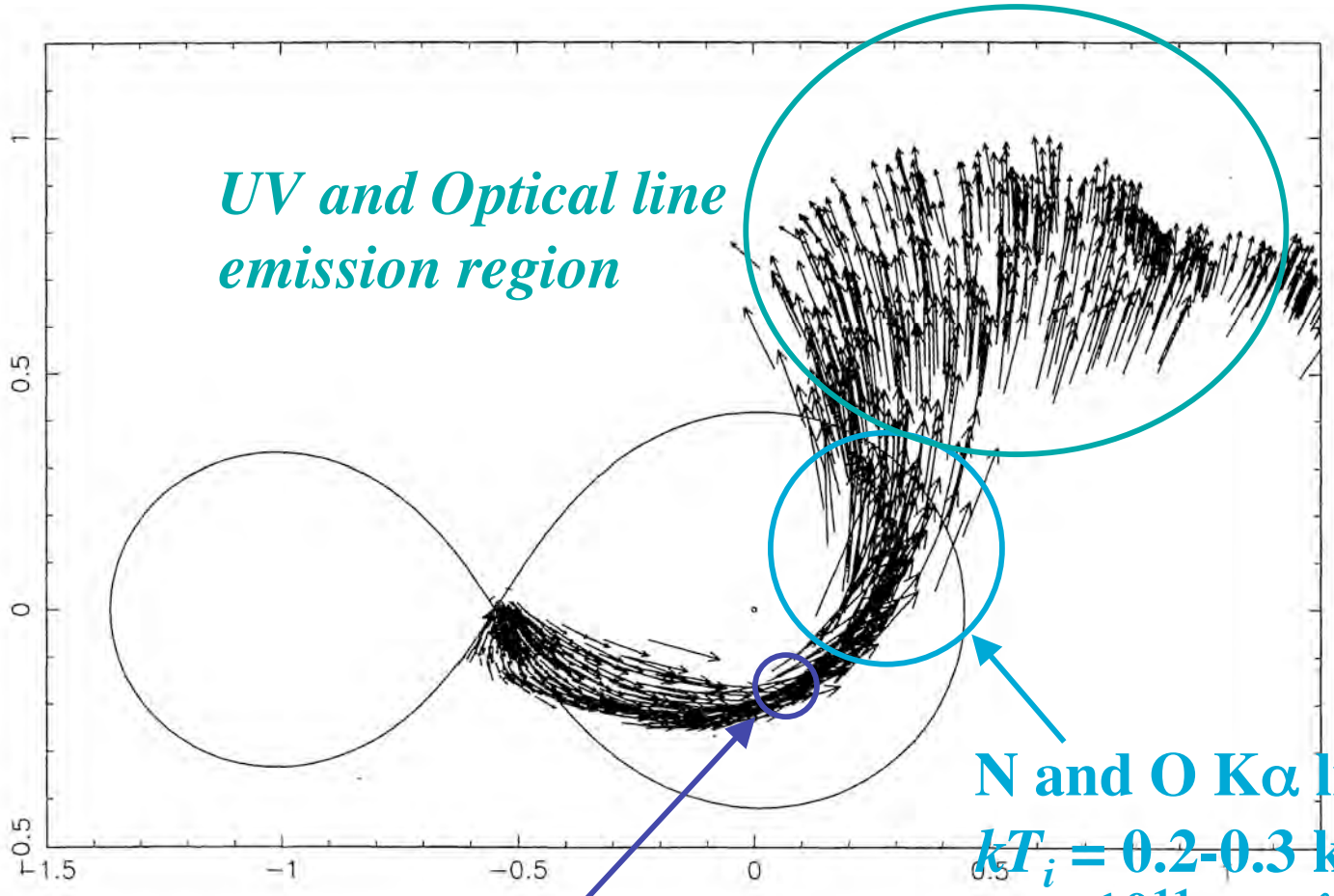

UV and Optical line emission region

N and O Kα line emission
kT_i = 0.2-0.3 keV
$n_e \sim 10^{11}$cm, $\ell_p \sim$ 2-3x10^{10}cm

Plasma heating
$r_{min} < 10^{10}$cm for kT_{max} = 4.6keV

Formation of millisecond pulsar

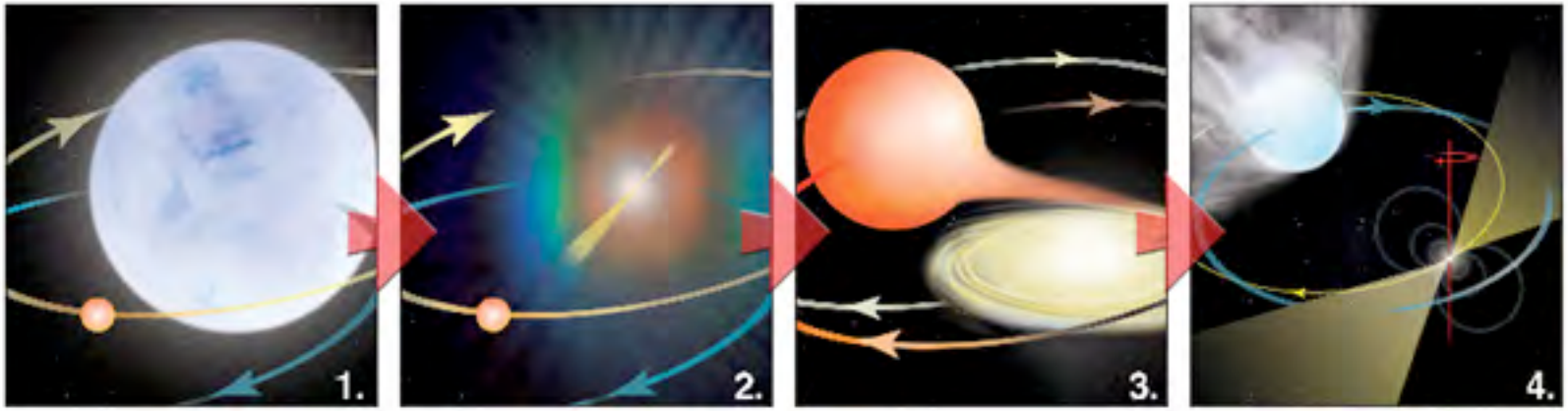

- Magnetized neutron star rotating at millisecond timescale.
- AE Aqr as a WD version of the millisecond pulsar at its formation.

X-ray Missions in the 21st Century

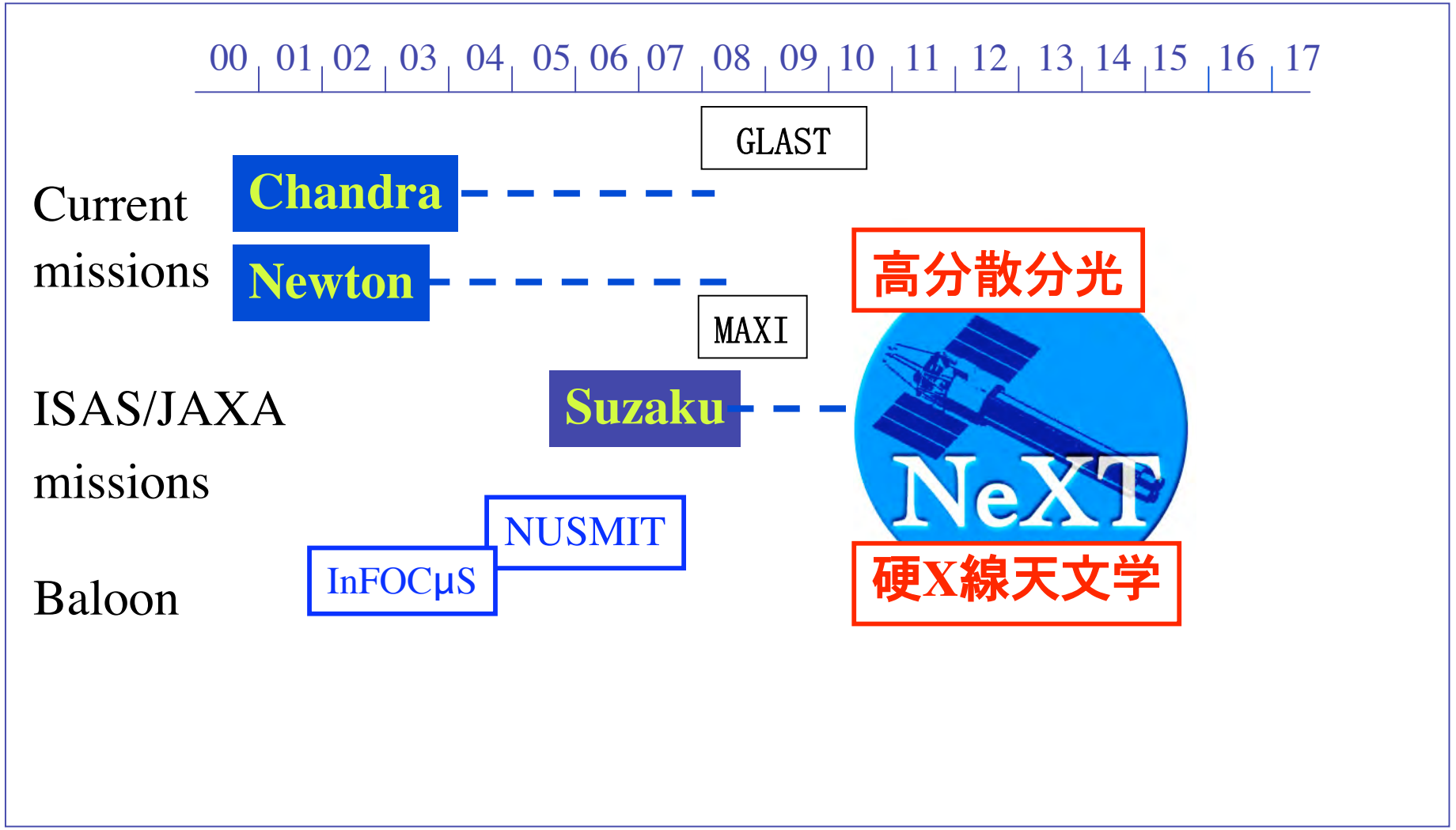

Spectrum of H-like/He-like iron K_α

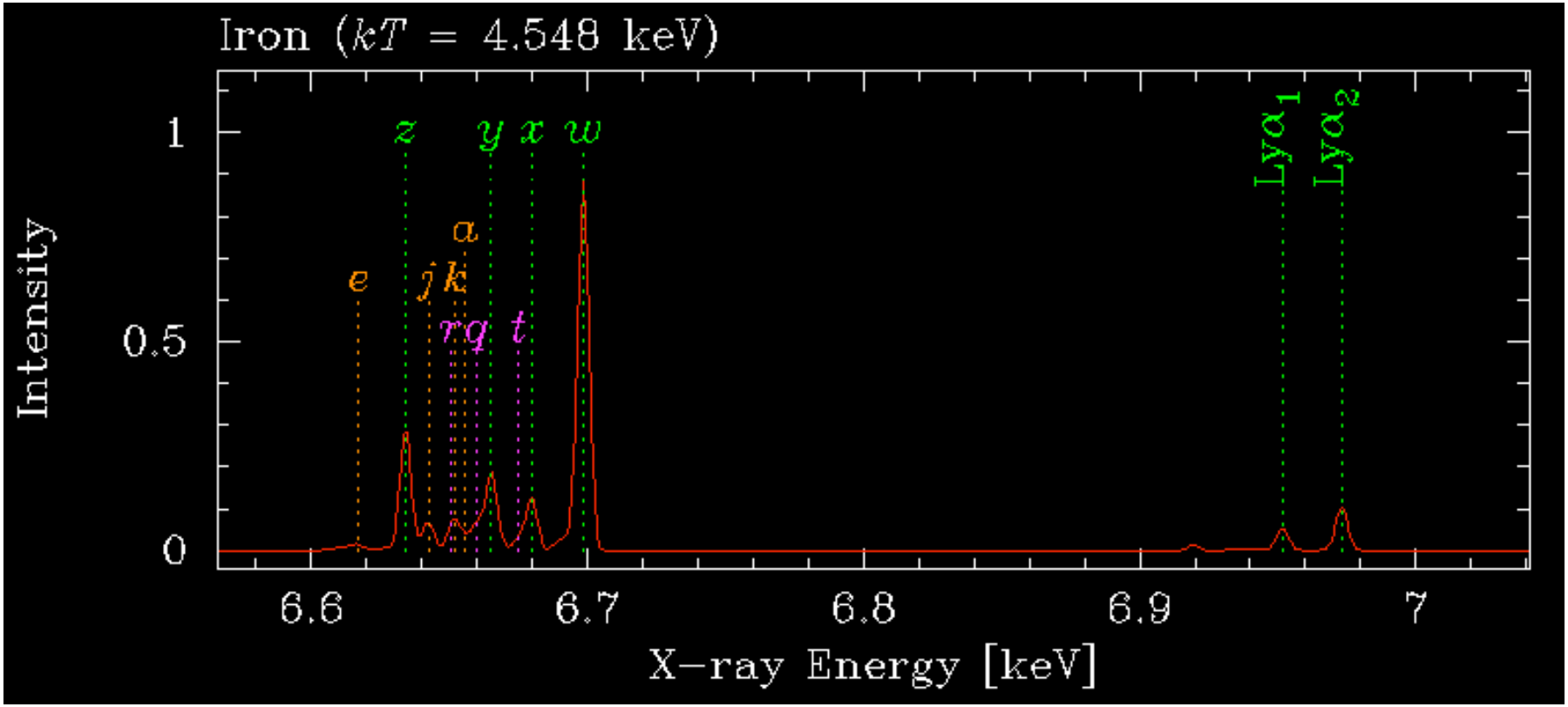

- Number of major satellite lines with spectator n=2 is 22.
- Spectator = 2p (DR): *a*, *b*, *c*, …, *m*, *n*: 14 in total.
  j and *k* are prominent
- Spectator = 2s (DR+IE): o, p, q, …, u, v: 8 in total.
  r, *q*, and *t* are strong in ionizing plasma

Intensity of the satellites with T_e

$kT_e = 1.6\text{keV}$

$kT_e = 3.2\text{keV}$

$kT_e = 7.9\text{keV}$